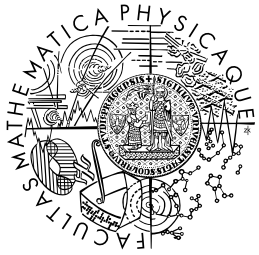

FACULTY
OF MATHEMATICS
AND PHYSICS
Charles University

BACHELOR THESIS

Adrián Sater

Laser pulse and source response on silicon detectors

Institute of Particle and Nuclear Physics

Supervisor of the bachelor thesis: RNDr. Peter Kodyš, CSc.

Study programme: Physics

Study branch: Nuclear and Particle physics

Prague 2022

I declare that I carried out this bachelor thesis independently, and only with the cited sources, literature and other professional sources. It has not been used to obtain another or the same degree.

I understand that my work relates to the rights and obligations under the Act No. 121/2000 Sb., the Copyright Act, as amended, in particular the fact that the Charles University in Prague has the right to conclude a license agreement on the use of this work as a school work pursuant to Section 60 subsection 1 of the Copyright Act.

In ..... date ....

Author's signature

Firstly i would like to thank my supervisor of this bachelor thesis, RNDr. Peter Kodyš,CSs., for valuable advice and supportive and friendly approach. Moreover, I would like to thank both my supervisor, and Mgr. Martin Sýkora for finding time to consult with me during writing of this thesis.

I am also very thankful to my girlfriend, friends and my family for supporting me during my study and never letting me give up.

My special thanks goes to my friend, Dominika Brezinová, for helping me with other subjects allowing me to dedicate more time for the thesis.

Title: Laser pulse and source response on silicon detectors

Author: Adrián Sater

Institute: Institute of Particle and Nuclear Physics

Supervisor: RNDr. Peter Kodyš, CSc., Faculty of Mathematics and Physics

Abstract: This thesis is focused on introduction on project CERN and ATLAS and on apparatus used for detection of particles. Moreover, thesis describes upgrades of detection apparatus, whose goal is to increase performance of the ATLAS detector(ATLAS Upgrade), these upgrades should result in increase of centre of mass energy in collisions and luminosity in collider, thus enabling new discoveries. Thesis also describes operation principle of silicon detectors and their utilization in ATLAS and ATLAS Upgrade. Subsequently, in third part of the thesis principle of measurement, data acquisition from measurements and data analysis is explained. The calibration of modules done before measurements is also described. In the last part, thesis focuses on describing various tests used for testing silicon sensors and their application in laboratories of Institute of Particle and Nuclear Physics in Prague. Unfortunately, thesis does not contain practical part in the form of tests on new chips as they were not ready until February 2022 and also the laboratory for laser tests was disassembled due to reconstruction.

Keywords: ATLAS Upgrade silicon detectors tests

Názov: Testovanie kremíkových detektorov laserom a žiaričom

Autor: Adrián Sater

Vedúci práce: RNDr. Peter Kodyš, CSc., Matematicko-fyzikálna fakulta

Abstrakt:

Predložená práca sa zameriava na zoznámenie sa s projektom CERN a ATLAS a s aparatúrou používanou na detekciu častíc. Ďalej sú v práci opísané vylepšenia detekčnej aparatúry ,ktorých cieľom je zvýšiť výkonnosť detektoru ATLAS, tzv. ATLAS Upgrade. Tieto vylepšenia by mali viesť k zvýšeniu energie zrážok a svetelnosti v urýchľovači, a teda umožniť nové objavy. V práci je taktiež vysvetlený princíp fungovania kremíkových detektorov a ich využitie v ATLAS a v ATLAS Upgrade. V tretej časti práce je vysvetlený princíp merania a získavania dát z meraní ako aj ich spracovanie. Taktiež je v tejto časti vysvetlená aj kalibrácia modulov pred meraniami. V poslednej časti práce je výklad sústredený na popis rôznych testov používaných na testovanie kremíkových senzorov a ich prevedenie v laboratóriách Ústavu časticovej a jadrovej fyziky v Prahe. Bohužiaľ, práca neobsahuje plánovanú praktickú časť v podobe testov na nových čipoch, nakoľko ich spojazdnenie bolo uskutočnené až vo Februári 2022 a aparatúra na testovanie s laserom je rozobratá z dôvodu prestavby laboratória.

Kľúčové slová: ATLAS Upgrade kremíkové detektory testy

Contents

Introduction

The European Council for Nuclear research, also known as CERN, is one of the world's leading institutions in particle physics. Originally established by twelve founding states, the CERN was supposed to answer questions about atomic nuclei but soon its focus was shifted on high energy particle collisions. The Large Hadron Collider is a part of this research centre with four detectors one of which is ATLAS.

Currently, the ATLAS detector is undergoing series of upgrades resulting in new structure called ATLAS Upgrade with higher luminosity and energy in particle collisions, thus creating environment suitable for new discoveries bringing us ever so closer to understanding universe. Laboratory of Institute of particle and nuclear physics in Prague is one of the centres helping with production of silicon modules scheduled to be used for particle detection in ATLAS Upgrade.

The main goal of this thesis was to introduce the function of ATLAS and its Upgrade as well as testing done, even in Prague, on silicon sensors and data acquisition. The first chapter gives brief overview of CERN and its Large Hadron Collider with its detectors combined with closer look at the functionality of ATLAS detector and the preview of ATLAS Upgrade project. Moreover, the chapter lists already done upgrades as well as ongoing ones with a brief description on what changes.

In the second chapter, the thesis focuses on semiconductors and a working principle of semiconductor detectors with their use in particle physics namely in ATLAS detector. The comparison of old SCT(ATLAS) and new ITk(ATLAS Upgrade) structure is made, explaining different types of modules and their layouts used in the structure.

The aim of the third chapter was to describe different parts of readout system in new ATLAS Upgrade with a trigger system ensuring event filtration. In addition to that used Hardware and Software were described concerning different types of chips and macros used for analysis. The end of this chapter was dedicated to calibration tests used to determine properties of tested module and to introduce preparation for termocycling tests in Prague with a goal to determine the durability of modules.

This thesis is concluded by explanation of special tests used for determining the functionality and properties of manufactured sensor. Chapter explains several methods used with their advantages and gives a description of its application in Prague laboratories.

Unfortunately, the thesis does not contain chapter with planned practical part of readout test on new star chips as at the time of thesis setup was unavailable due to reconstruction of laser test laboratory and late arrival of modules with mentioned chips.

1. CERN

The acronym **CERN** is originally from french **C**onseil **E**uropéen pour la **R**echerche **N**ucléaire which stands for European Council for Nuclear research[1], established by 12 European founding states in 1952. Laboratory's original devotion was on study of atomic nuclei, but was soon changed to high-energy physics, focusing mainly on interactions between subatomic physics.

The CERN laboratory, as we know it today was founded in 1954 and is located in Franco-Swiss border near Geneva. It has 23 member states. Nowadays CERN's role is to provide the particle accelerators and other infrastructure for high-energy physics research. CERN is also a site of the Large Hadron Collider (LHC) which is world's largest particle collider.

Physicists and engineers use these scientific instruments provided by CERN to study the basic constituents of matter (fundamental particles). Subatomic particles are made to collide at the speed close to speed of light. This process gives us valuable information about the interaction of particles thus giving us insight into the laws that our world abides by. The study of high-energy collision is made possible by **particle accelerators** and **detectors**, we will talk about them later in the upcoming paragraphs.

CERN was behind many scientific discoveries, some of include discoveries such as:

- The discovery of W and Z bosons in the UA1 and UA2 experiments.
- The first creation of antihydrogen atoms in the PS210 experiment.
- Discovery of a boson with mass around 125GeV/c^2, Higgs boson.

For the latest of mentioned, the scientists F.Englert and P.Higgs were awarded the 2013 nobel prize for physics.

1.1 LHC

The Large Hadron Collider is the world's largest and most powerful **particle collider**. The LHC is a proton-proton collider with 14TeV centre of mass energy. Its first start is dated to 10. September 2008, and remains the newest addition to CERN's accelerator complex. The LHC is composed of 27-kilometre ring of superconducting magnets with several structures whose purpose is to boost the energy of the particles before collision.[2] The figure 1.1 shows the accelerator complex.

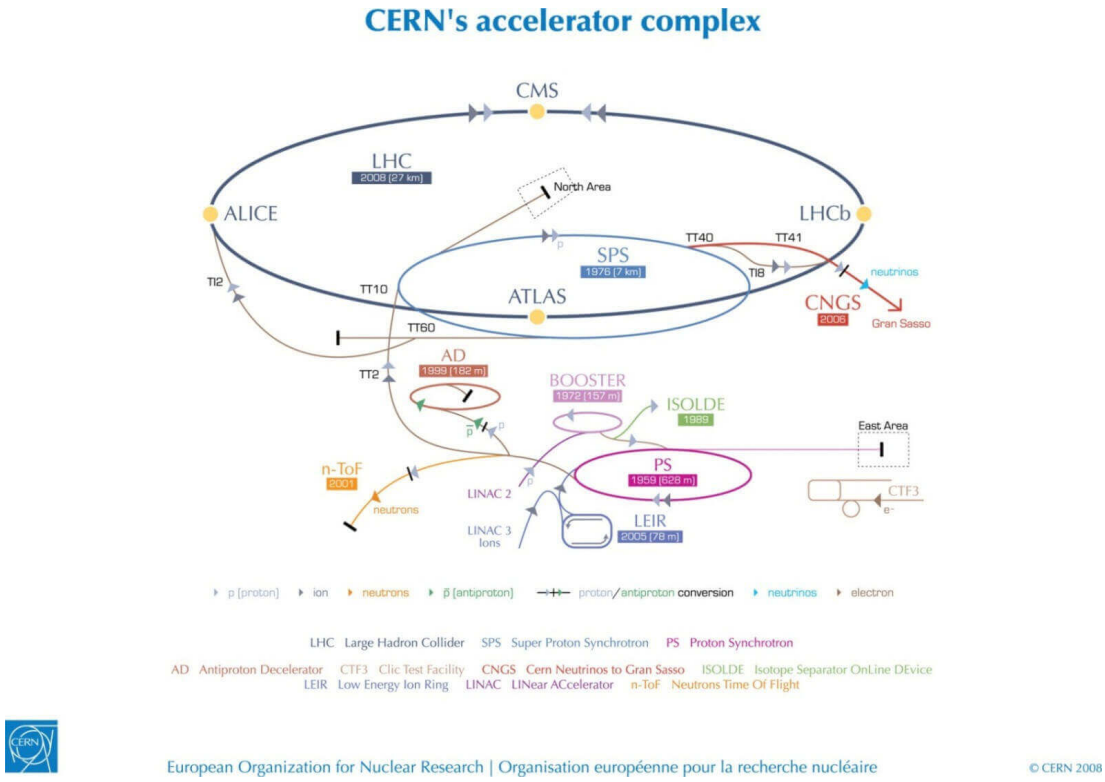

Figure 1.1: Cern's accelerator complex [3]

Inside the LHC two particle beams travel in opposite directions. Their direction is maintained by super-conduction electromagnets which are build from coils operating in superconducting state. The entire control of this process is housed in the CERN control centre. The place of collision is chosen in consideration of the positions of particle detectors :

- ATLAS - A Toroidal LHC Apparatus
- CMS - Compact Muon Solenoid
- ALICE - A Large Ion Collider Experiment
- LHCb - Large Hadron Collider beauty

Large Hadron Collider opens new frontier in particle physics due to its high energy collisions, as well as provides high-accuracy measurements of known objects. The collider was built to help scientists to answer several key questions in particle physics. Some of them are:

- What is the origin of mass?
- Why do some particles have mass at all ?
- What is mass ?
- What is dark matter ?

Some of these questions are being explained by the work of scientists at the CERN. There were also made some groundbreaking discoveries, as the discovery of Higgs boson which is essential for standard model to work.

1.2 ATLAS

ATLAS is a cylindrical detector with dimension of 46 meters in length and 25 meters in diameter weighting 7000 tones. It is located 100 meters under ground and could be described as complex tool designed to detect some of the tiniest particles. The ATLAS experiment was constructed in order to observe and study physics of high velocity collisions of particles. Inner detector, situated in centre of ATLAS detector is responsible for tracking the colliding particles. It consists of pixel detector, surrounded by semiconductor tracker of which functions we will talk later in the thesis. The figure 1.2 shows detector ATLAS.

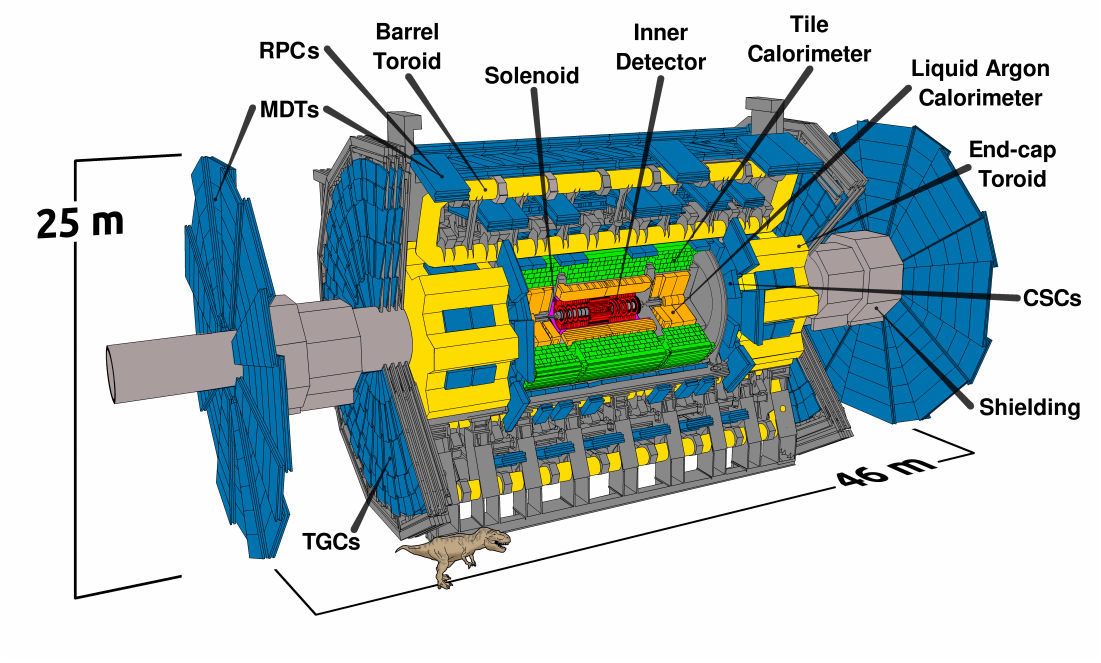

Figure 1.2: Detector ATLAS [4]

It is composed out of 6 different concentric subsystems in layers around the collision point. Out of these subsystems we have four main sub-detectors, which will be discussed later:

- Inner detector
- Electromagnetic calorimeter
- Hadronic calorimeter
- Muon spectrometer

Whole system is used to measure trajectory, momentum and energy of particle. These information then allow us to individually identify the particles. Precision of momenta measurements are obtained by huge magnet system which bends the paths of the particles with charge.

The detector has a cylindrical symmetry due to the nature of collision. Collision debris is produces in the place of impact of two high-energy beams of

particles. The debris are new particles, formed by the impact, flying in all directions. In order to detect as much particles as possible we need to create detector with maximal surface, therefore cylindrical symmetry. The detector has a variety of usages ranging from study of Higgs boson to the search of new dimensions.[5]

1.2.1 Inner Detector

Inner detector is placed inside of the cylinder closest to the collision in a solenoidal magnetic field of 2 T. Its dimensions are 7m length and a radius of 1.15m. Inner detector has two parts where the inner part measurements of pattern recognition, momentum and vertices as well as electron identification are achieved by the combination of semiconductor pixel and strip detectors, whereas in the outer part it is done by straw-tube tracking detectors with transition radiation capability. The Figure 1.3 depicts Inner detector, detector closest to collision.

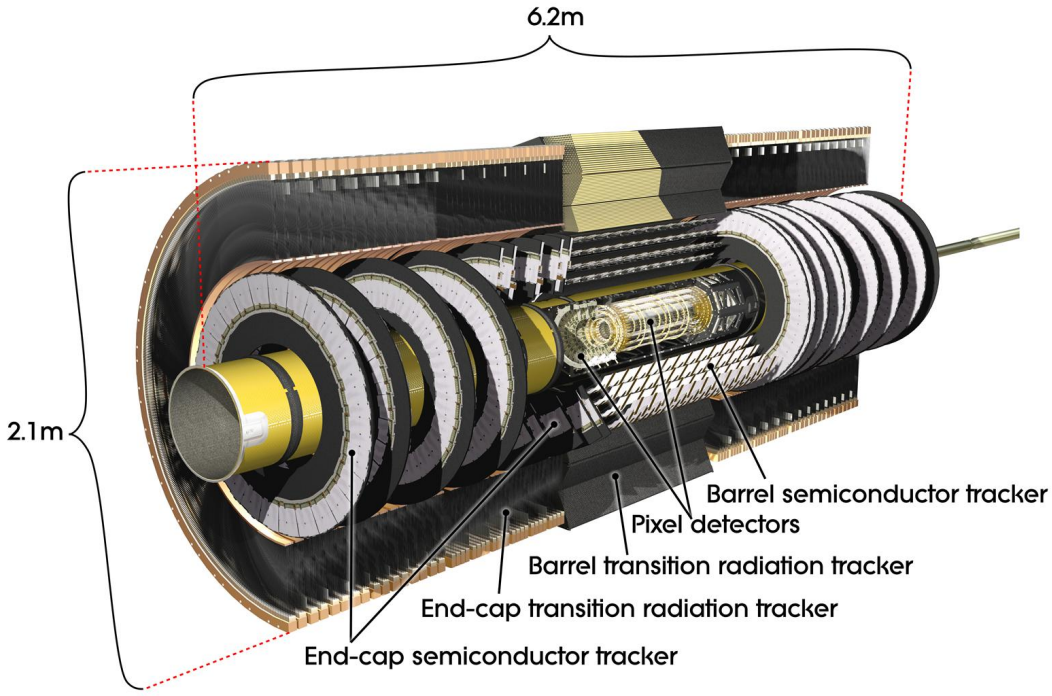

Figure 1.3: Inner detector [6]

The purpose of pixel detector is to provide set of measurements as close to the place of collision as possible. There are as much as 140 million pixel detectors in the shape of rectangle with the surface of 50x300μm. The thorough principle of Semiconductor tracker (SCT) and strip detector will be discussed later but in a nutshell: SCTs function on the principle of ionization of the silicon by passing of charged particle resulting in creating of electron-hole pairs which are then detected on electrodes. At last the Transition Radiation Tracker(TRT) uses xenon gas to detect transition-radiation photons for electron identification. Barrel contains about 50000 straws each with 4mm in diameter equipped with 30μm diameter gold-plated wire.[7]

1.2.2 Calorimeters

As we travel closer to the surface of detector we meet calorimeters, electromagnetic and hadron. The main goal of the calorimeters is to absorb most of the particles from collision, forcing them to stop inside the detector and give up their energy. Not only they absorb the particle, the part of calorimeters, called active medium, determines the energy of absorbed particle.

Electromagnetic calorimeters(EM) are designed to stop and measure energy of electrons and photons using their interaction with matter. Detection of particle in EM is provided by Liquid Argon calorimeter(LAr) where metal layers absorb energy of incoming particles turning them to lower energy particles. These ionise liquid Argon creating measurable current. Energy of absorbed particles can be determined by combining these currents.

In contrary, Hadron calorimeters use interaction with atomic nuclei to stop hadrons(particles containing quarks). Tile hadronic calorimeter, surronding LAr, functions on same principle as LAr: Parcticles that didn't deposit all of their energy in LAr are turned into particles with lower energy by hitting the steel layer. This results in scintillators producing photons which are then converted to current.

We can identify absorbed particle by knowledge of the layers on which it stopped. Calorimeters can stop most of the particles apart from neutrinos and muons.[8] The Figure 1.4 depicts positions of calorimeters in ATLAS detector.

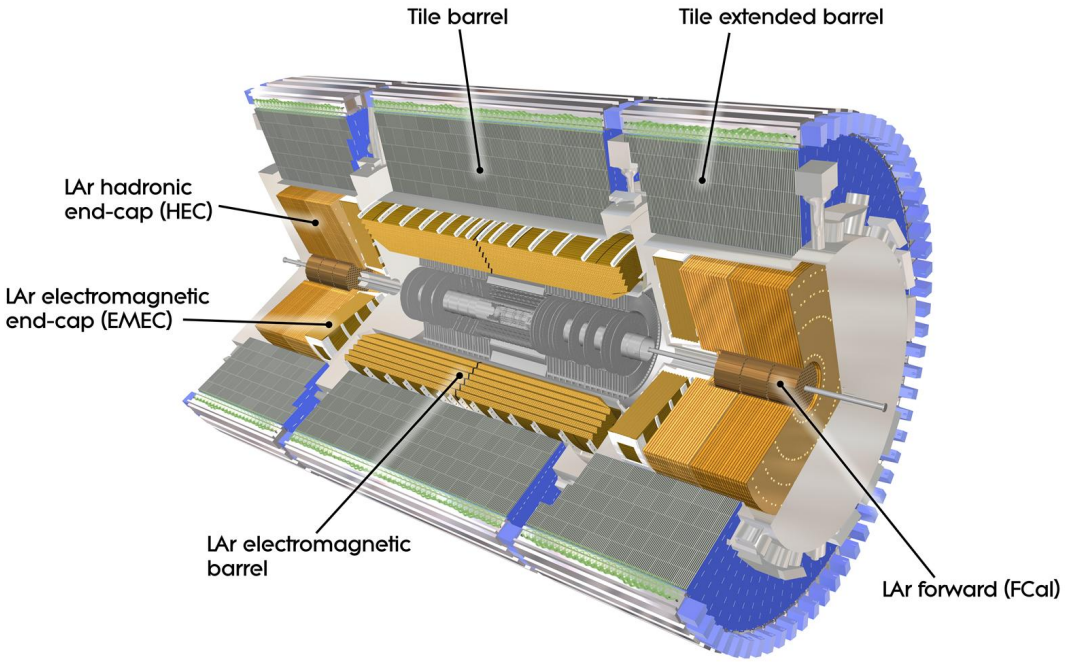

Figure 1.4: Calorimeters in Detector ATLAS [8]

1.2.3 Muon spectrometer

Muon spectrometers are used for detecting particles that pass through all the previous layers. The muon spectrometer in ATLAS is constructed out of 4000 individual muon chambers using 4 sub-parts for detection[9]:

- Thin Gap Chambers - triggering and also for measurement of the second coordinate. Located at the ends of the detector.
- Resistive Plate Chambers - same as thin gap chambers but are located in center region.
- Monitored Drift Tubes - measuring trajectory.
- Cathode Strip Chambers - measures precision coordinates. Located at the ends of detector.

The figure 1.5 shows muon spectrometer in ATLAS.

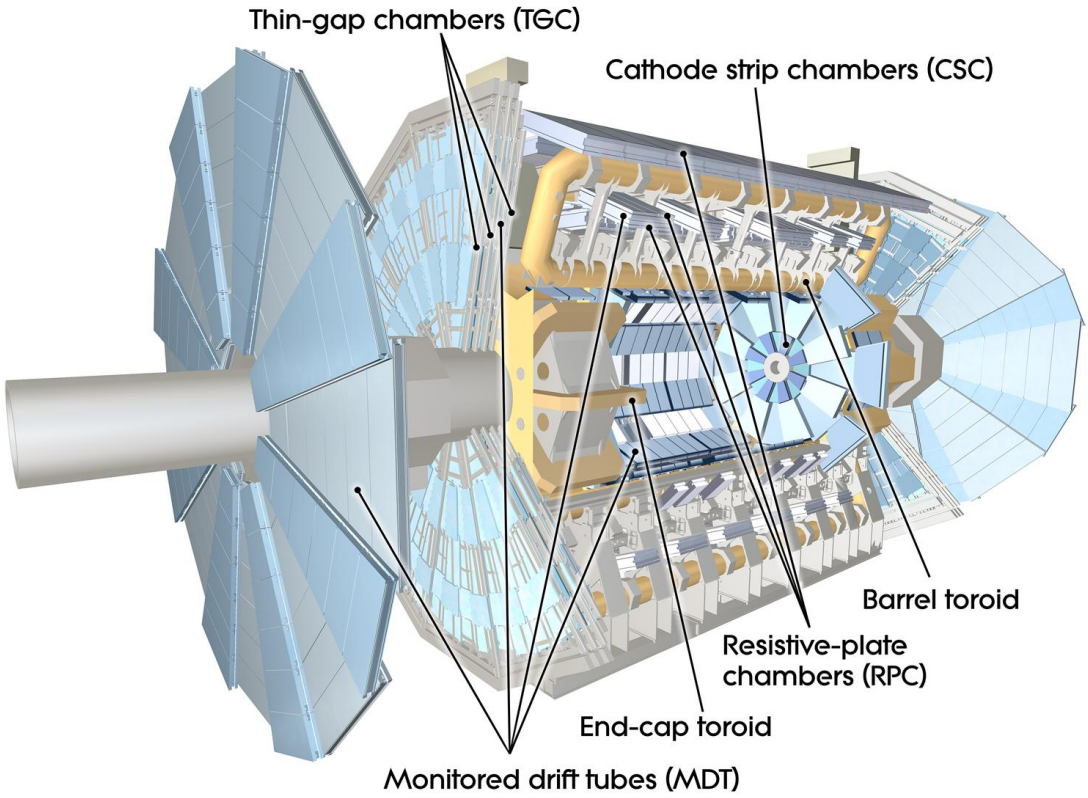

Figure 1.5: Muon spectrometer [9]

1.2.4 Trigger system

Another part of ATLAS detector is the trigger system. Its main purpose is to distinguish important events that might include interesting physics. ATLAS observers enormous number of collision, but not all of them contain interesting information usable for further discoveries. Trigger or the selection of important

data works on two levels. The first-level is a hardware trigger which is located on the detector. It is based on set of information from calorimeters and spectrometer. The decision to keep or remove the data needs to be made in just 2.5 milliseconds. The second-level is a software trigger which uses the power of 40000 CPU cores for detailed examination of collision events send from first-level trigger. It selects the final set of data which are sent for further offline analysis.[10]

1.2.5 Magnets in ATLAS

The purpose of magnets in the ATLAS detector is to bend charged particles around various layers of detector. By bending the trajectory of these particles, we are able to determine their charge and momentum. The bending in ATLAS is accomplished by two types of superconducting magnets[11]:

- **Solenoidal** - located in the core of experiment surrounds inner detector. With its dimensions of 5.6m in length and 2.56m in diameter and weighting 5 tonnes it provides a magnetic field of 2 Tesla. This is fulfilled by over 9 km of superconductor wire.
- **Toroidal** - toroidal magnet provides magnetic force used for measurement of momentum of muons. This magnetic force of up to 3.5 T is created by series of eight coils. ATLAS contains 3 toroid magnets: two at the ends, and one surrounding experiment.
  - Barrel Toroid - largest toroidal magnet constructed with dimensions of 25.3m in length, weighting about 830 tonnes uses over 56km of superconducting wire.
  - End-cap Toroid - At 10.7m weighting 240 tonnes extends magnetic field to particles leaving the detector.

The figure 1.6 shows Barrel (left) and Toroidal (right) magnets in ATLAS.

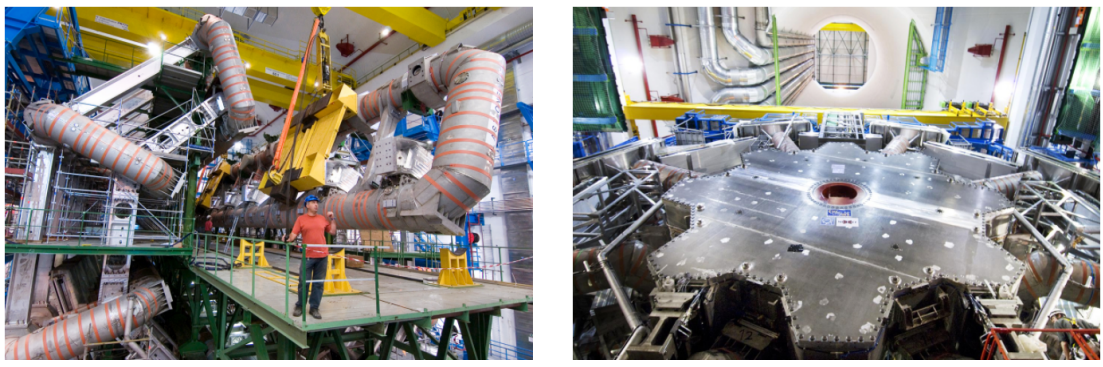

Figure 1.6: Magnets in ATLAS [11]

1.3 ATLAS Upgrade

Detector ATLAS will undergo several upgrades in order to enhance detecting abilities and also to maintain highest possible performance. These changes are

a result of radiation damage but also the everlasting desire to understand the nature. The said upgrade is being implemented in three "phases". Before the start of the upgrade process during the two year period (2011-2013) the ALTAS experiment has recorded proton-proton collisions up to 8 TeV at the centre of mass energy. During phase 0 upgrades the centre of mass energy in pp collision increased up to 13-14 TeV. The phase 1 concerns 4 areas of ATLAS detector[12]:

- **New Small Wheel detector**
- **Front-end electronics of Liquid Argon calorimeter**
- **Muon detectors**
- **Trigger and data acquisition system (TDAQ system)**

The phase 2 will affect:

- **Pixel and strip tracker**
- **LAr and Tile calorimeters**
- **Muon system**
- **TDAQ system**

1.3.1 Phase 0

The LHC already underwent an upgrade with increase of center of mass energy in proton-proton collisions and also the increase of peak luminosity. This upgrade took place in shutdown period 2013-2015. After the upgrade LHC continued gathering data on proton-proton collisions. The further phase 0 upgrades were[13]

- **New Aluminum beam pipe**
- **Additional new layer of pixel detectors**
- **Low voltage power supplies redesigned for the calorimeter front**
- A**Additional neutron shielding**

1.3.2 Phase 1

The work on this upgrade started in 2015-2016 and finished in 2017. Upgrades that were scheduled to take place in phase 1. [12]:

- **The New small Wheel system** - consists of two 5 meter radius wheels in the end-cap region aiming to reduce muon triggers caused by noise or accidental coincidences.
- **LAr calorimeter front-end electronics** - allowing us to increase trigger tower granularity and to maintain good trigger performance at high luminosity and pile up.

- **Muon detectors in the Barrel Inner Small region** - new resistive plate chambers were installed in order to cover previously not covered regions of pseudo-rapidity. Hopefully, resulting in reducing the foreseen moun trigger.

- **TDAQ system** - several upgrades are planed for TDAQ system in order to keep trigger rates at sustainable levels and guarantee smooth data taking despite the higher number of collisions. Some of the upgrades which will be performed: New Sector Logic board for the end-cap, Central Trigger processor, new readout system based on FELIX system.

These upgrades are designed to enable ATLAS experiment to fully exploit the physics opportunities provided by further luminosity increase. The ATLAS physics program put an emphasis on measuring properties of the newly discovered Higgs boson. The phase 1 upgrade was intended to confirm if the observed resonance is predicted Higgs boson, followed by precise measurements of its mass, width, production rates, branching ratios and its couplings to fermions and bosons. The experiment was also prepared for a further search for a new phenomena and new particles predicted by theoretical models such as supersymetry, compositeness, technicolor, extra-dimensions[13].

1.3.3 Phase 2

Upgrades scheduled to take place in phase 2[12]:

- **Pixel and Strip Inner trackers (ITk)** -mentioned later 1.4

- **LAr and Tile calorimeters** - as current liquid argon calorimeter electronics is not compatible with Phase 2 requirements, phase 1 boards will be kept but new front-end and back-end electronics will be installed allowing full granularity data to be sent off-detector at 40 MHz. Furthermore, tile calolimeter will undergo complete replacement of on-detector and off-detector electronics due to radiation damage.

- **Muon system** - aimed to reduce not muon originating triggers and to increase geometrical coverage in the barrel. In order to attain these upgrades new detectors will be installed in Small, Large sectors and thin Gap Chambers.

- **TDAQ system** - consisting of Level-0 Trigger, the Data acquisition and Event filter will be completely upgraded.

The phase 2 upgrade, currently in its final stage, is scheduled to take place in 2025-2027 time frame. Even further increase in luminosity up to $5\text{x}10^{34} cm^{-2} s^{-1}$, is supposed to provide valuable tool in reduction uncertainties in measurements of Higgs boson as well as extending the reach for new physics beyond the Standard model, including supersymetry and extra-dimensions, which can be achieved by studies of rare processes of the top quark[13].

1.4 ATLAS Upgrade inner tracker (ITk)

The current ATLAS inner detector was designed to last for 10 years and withstand lower luminosity and lover pile-up. Therefore, due to the High radiation, and also in order to prepare for higher pile-up, the old Inner detector is being replaced by new, all-silicon, Inner Tracking System(ITk), as it also needs to prepared to measure higher multiplicity of collisions. Therefore ITk has $13m^2$ of pixel detectors with 5 billion readout channels and $160m^2$ of strip detectors with 50 million readout channels. The biggest difference between old and new inner detector is that the TRT is being completely replaced by addition semiconductor long strip layers as TRT would not withstand higher luminosity pile-up.[14] The layout of active elements in the ITk detector is shown in 1.7 with a comparison to older Inner detector SCT layout 1.8.

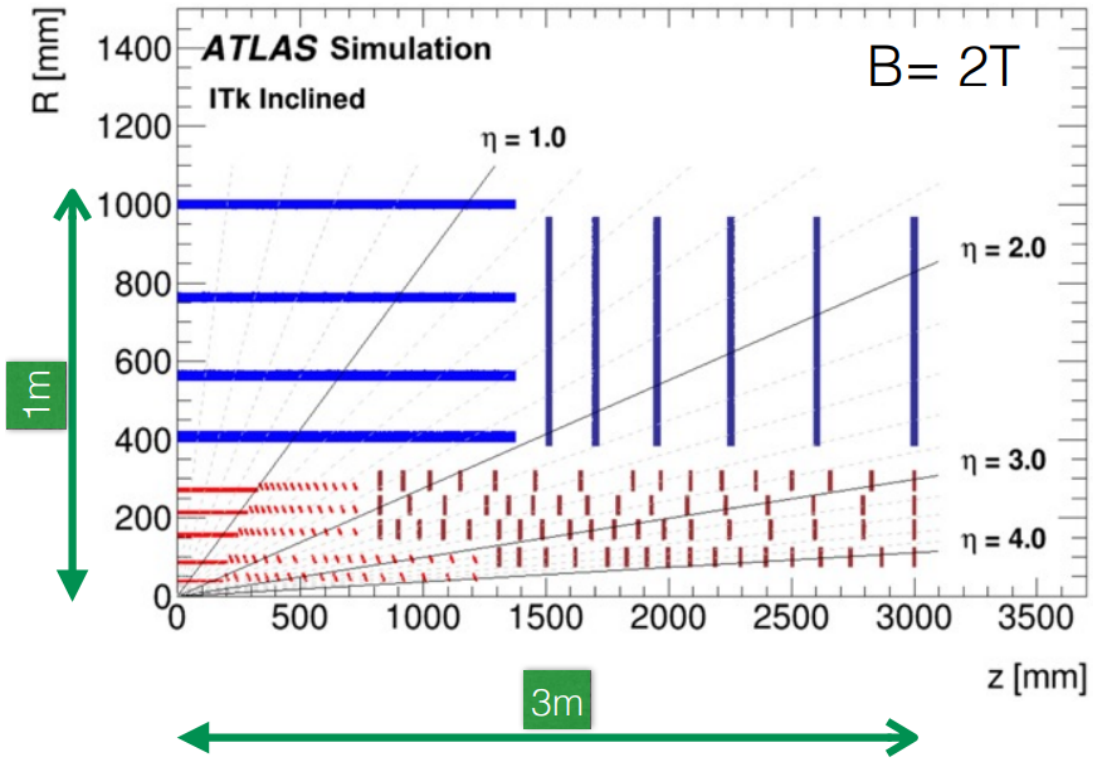

Figure 1.7: Layout schematic of ITk [15]

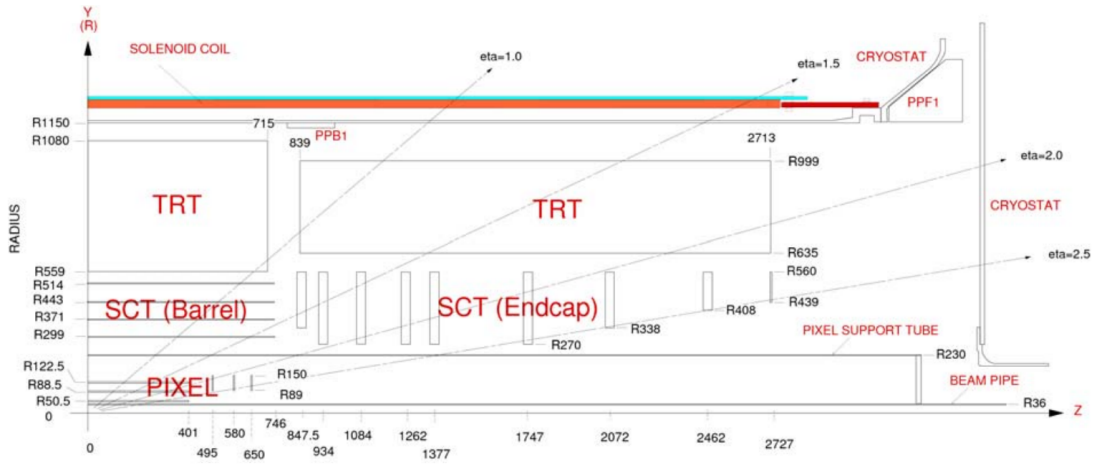

Figure 1.8: View of the older ATLAS Inner detector(before ATLAS Upgrade) [21]

2. SCT and ITk

2.1 Semicondutors

Semiconductor trackers, also known as SCTs, are located in ATLAS Inner detector surrounding pixel detectors. Mostly used material in construction of these trackers is silicon. Silicon is a semiconductor, element defined by its conductivity properties which are between the conductor and insulator. Their conductivity and other properties can be altered with he introduction of impurities, to meet a specific needs. Therefore semiconductors can be divided into two types: intrinsic and extrinsic.

2.1.1 Intrinsic semiconductors

In intrinsic semiconductor, at temperature above absolute zero, there is a finite probability electron in lattice will be knocked loose from its position, leaving behind an electron deficiency called hole. By further applying voltage, both loose electron and hole can contribute to a small current flow. The current in an intrinsic semiconductor consists of both electrons and holes.[16]

2.1.2 Extrinsic semiconductors

Extrinsic semiconductors are made by adding (doping) intrinsic semiconductor with chemical impurities. This change is achieved by doping atoms of different elements into the sample. These impurities affect conductive properties of the sample. In comparison to intrinsic semiconductor the number of free electrons and holes contributing to current is not equal. Extrinsic semiconductors can be further divided into two groups:

- n-type - donor impurity atoms have more valance electrons than the atoms of sample. Resulting in increase of negative charge carrier thus n-type. An n-type semiconductors are made by adding atoms from Group-V (five electron in valance band) elements to the intrinsic semiconductor(Group-IV)

- p-type - acceptor impurity atoms have less valance electrons as atoms of the sample. By accepting electrons from the sample number of positive charge carriers increases thus p-type. A p-type semiconductors are made by adding atoms from Group-III (three electron in valance band) elements to the intrinsic semiconductor(Group-IV).

The Figure 2.1 shows energy bands in semiconductors and figure 2.2 represents types of doping.

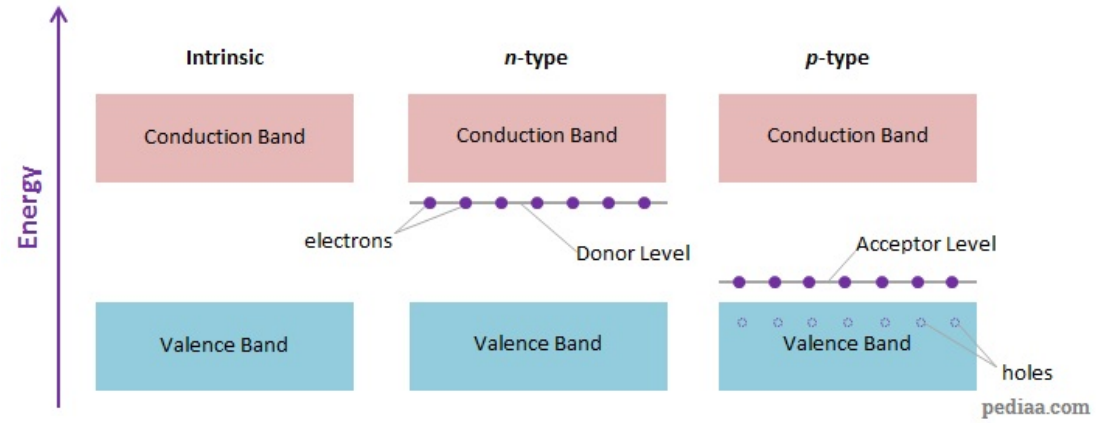

Figure 2.1: Energy bands in semiconductors [17]

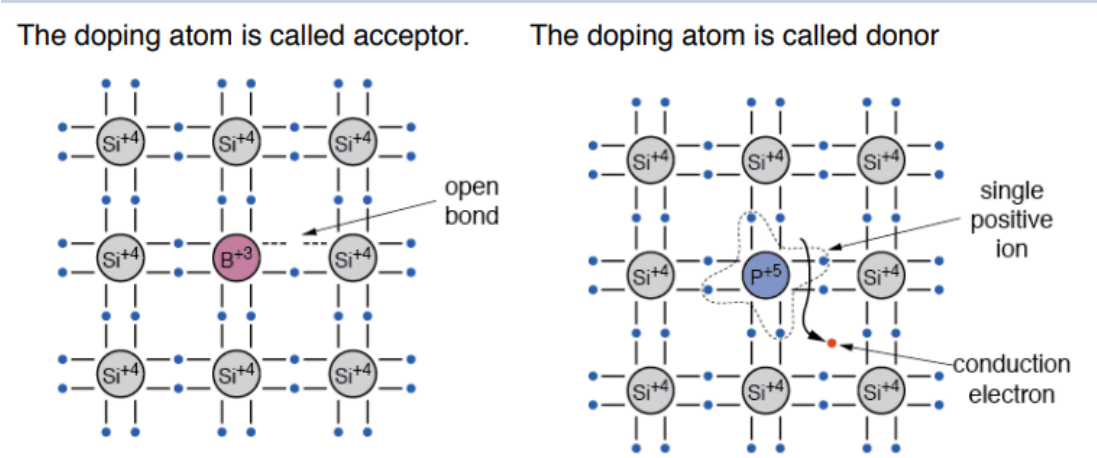

Figure 2.2: Creation of Extrinsic semiconductors by doping [18]

2.2 Silicon detectors

2.2.1 Detection principle

Majority of silicon detectors work by doping narrow strips of silicon to turn them into diodes (putting p-type and n-type together). The detection principle lies in so called p-n junction. This p-n junction can be connected to the current in reverse biased or forward biased mode. Namely the reverse biased mode is used in detection of particles. By connecting p-n junction in reverse biased mode we create so called "depleted region" as holes in p-type are pulled away from junction by negative terminal. On the other hand, the electrons from n-type are pulled away from the junction by positive terminal. This creates the mentioned depleted region which then acts as sensitive detector for particle detection. When charged particle passes through the silicon it ionises atoms in the crystalline lattice around its path. Resulting in creating pairs of electrons and holes which are then collected

by electrodes and we detect current. By creating a detector with many of these strips and dividing them into regions we can get a pretty accurate picture of the path of particle. The Figure 2.3 depicts cross section through the strip detector.

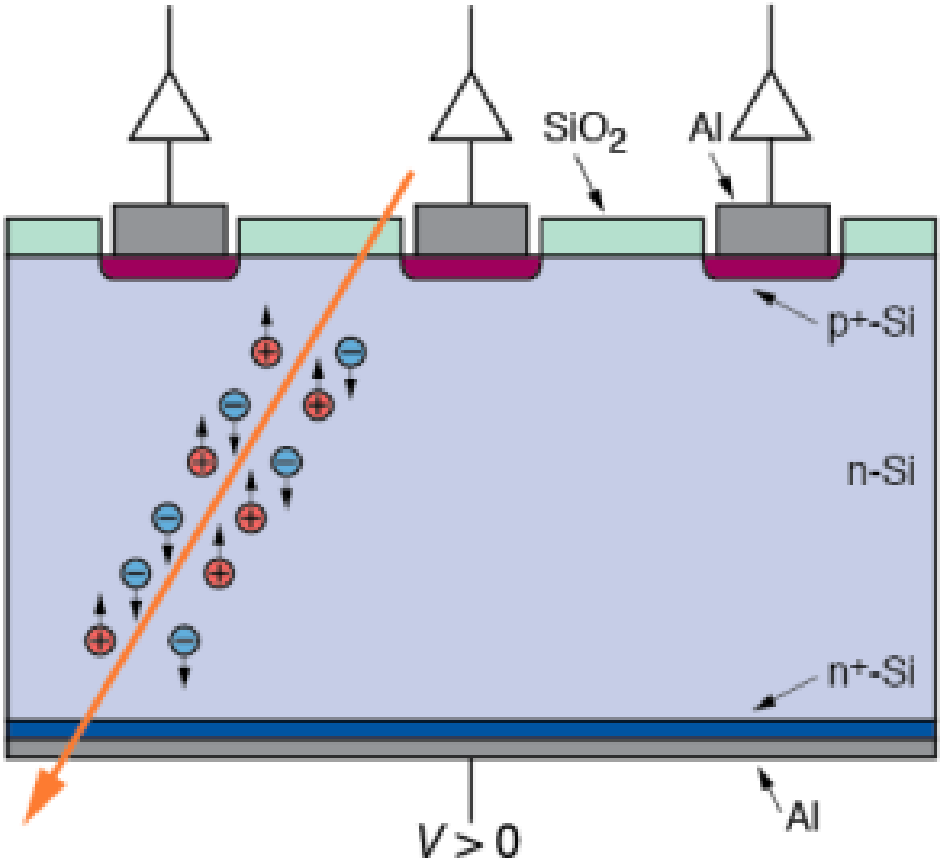

Figure 2.3: Cross section through the strip detector (p-type) [18]

2.2.2 Usage of detectors

There are several possible usages of silicon detectors. These detector can be used on position measurement, energy measurement or radiation level measurement. We will closely discuss those used on position measurement as this is their purpose in ATLAS detector. Types of position sensitive detectors used in ATLAS/ATLAS Upgrade are silicon semiconductor detectors. The principle of detection was discussed in earlier section. The idea behind its detection is that particle passing through depleted zone ionises and creates electron-hole pair resulting in electrical impulse in the circuit.

2.3 SCT in ATLAS

SCT or semiconductor tracker in ATLAS consists of microstrips which are arranged into barrel made of four cylinders and two endcaps made our of nine

disks. Microstrip detectors are electrodes divided into number of independent segments or strips. Electron-hole pairs created by ionization then travel to corresponding segments, allowing us to determine place of interaction by the strength of the signal. The cylinders carry the total number of 2112 identical detector units(barrel modules)[19]. The table 2.4 shows parameters of SCT in ATLAS.

Barrel cylinder	**r (mm)**	**Tilt angle (deg)**	**Modules**
B3	299	11	384
B4	371	11	480
B5	443	11.25	576
B6	514	11.25	672
		total	2112
Endcap disk	Inner r (mm)	Outer r (mm)	Modules
1,7	337	560	92
2,3,4,5,6	270	560	132
8	408	560	92
9	439	560	52
		total	1976

Figure 2.4: Table of SCT parameters [19]

2.3.1 Barrel modules

Barrel modules consist of baseboard, four microstrip sensors, and an electronic hybrid wrapped around centre of module. Major design parameters of barrel module are:

- **Sensors** - 63.56x63.96mm^2
- **Strips** - 80µm pitch (Pitch is distance between two adjacent strips), 126mm length
- **Operation temperature** -7°C

The picture 2.5 shows 3D view of mentioned Barrel module.

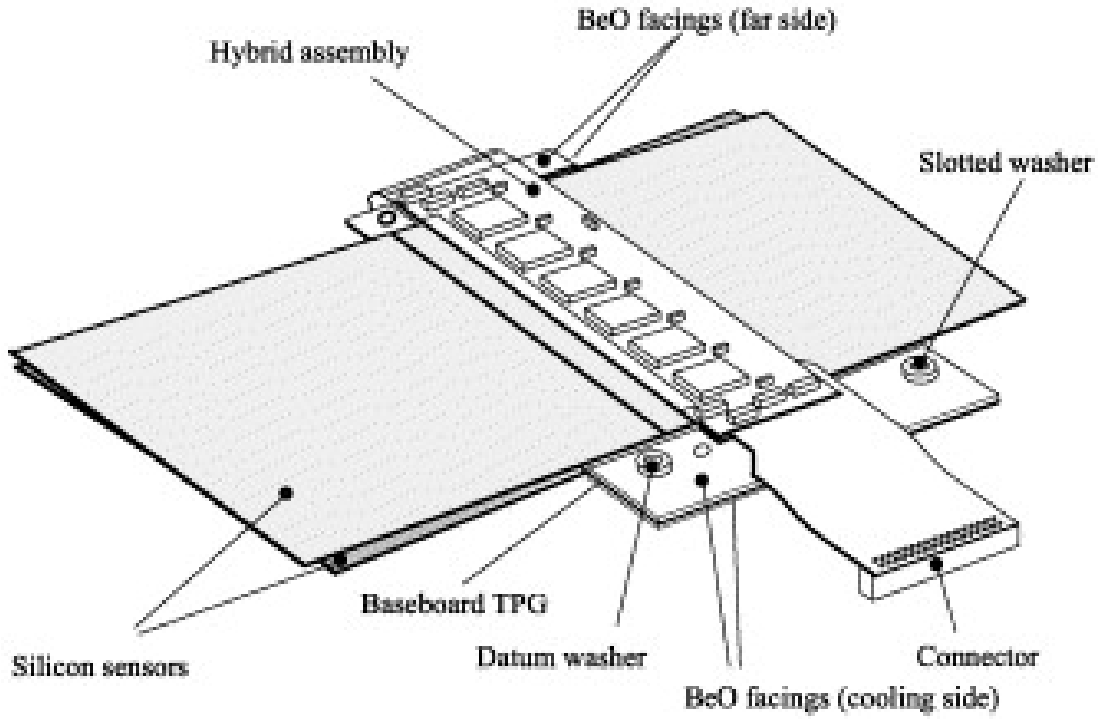

Figure 2.5: Barrel module [19]

Let us now take a look at functions of some fundamental individual components of barrel module [19][20]:

- **Baseboard** - made of Thermal Pyrolytic Graphite (TPG), provides mechanical structure, thermal conductivity heat path as well as electrical connection to the backside of the sensors.
- **Hybrid** - made out of four layers of printed circuit, reinforced mechanically, thermally, and electrically with carbon substrate, carries 12 readout ASICs (Application Specific Integrated Circuits). Connections between sensor pairs, sensors and hybrid and between ASICs and hybrids are made by aluminium wire-bonds.
- **Microstrip sensors**- are part of the barrel as well as end-cap detection modules in the SCT. There are mostly two single-sided sensors on each side of module glued around high thermal conductivity substrate.

View of the ATLAS Inner detector before upgrade can be seen on figure 1.8

2.3.2 End-cap modules

As we have already mentioned, the old ID(Inner detector) consisted of both barrel and end-cap regions in order to minimize material seen by traversing particles. End-caps consist of 9 disk layers. The number of modules in a given ring was determined in the process of defying the module geometries with the goal of minimizing costs, resulting in largest sensor geometries that could be accommodated.

Modules can be divided into 3 categories according to their position a these are constructed out of different sensor types[21]:

- Inner - W12
- Middle - W21 + W22: In middle region, namely in 8th disk the geometry needed would require to cut a standard middle module in half so in order to reduce costs short-middle module was introduced using only W22 sensor.
- Outer - W31 + W32

The figure 2.6 shows layout of different types of end-cap modules.

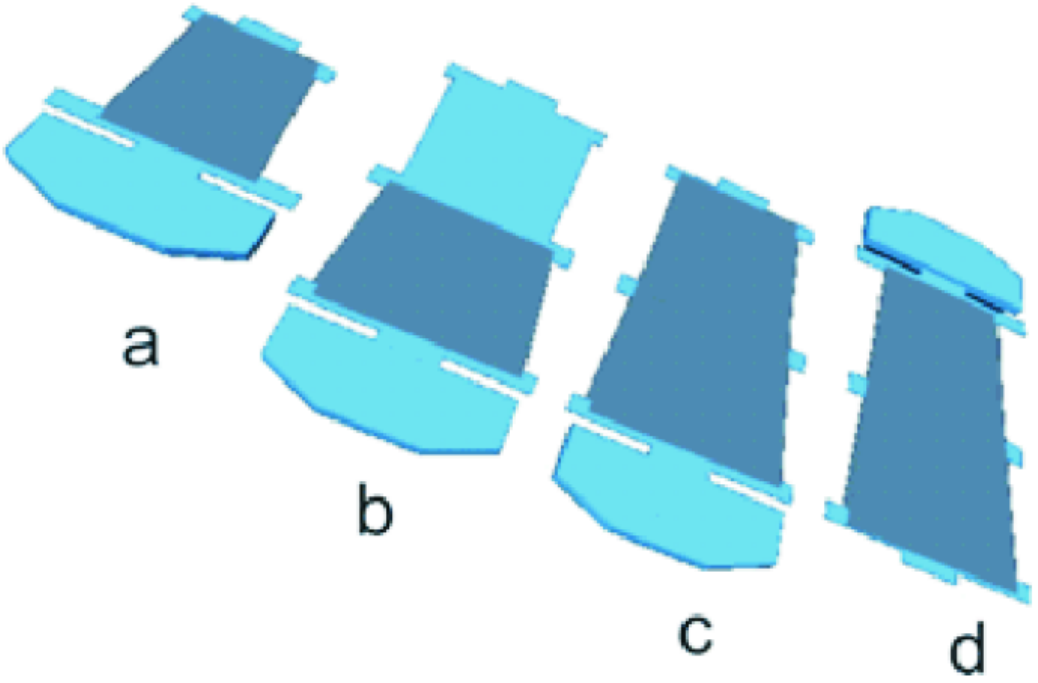

Figure 2.6: Layout of end-cap modules in SCT in Athena framework: (a) inner, (b) short-middle, (c) middle, (d) outer [21]

Some of the Sensor parameters can be seen in Table 2.7.

Module	Sensor Type	Sensor Centre mm	½ length mm	Rin mm	Rout mm
Inner	W12	304.550	29.5500	275.00	334.10
Middle	W21	369.163	31.5625	337.60	400.73
	W22	429.063	26.2375	402.83	455.30
Outer	W31	470.555	31.7900	438.77	502.35
	W32	532.223	27.7775	504.45	560.00

Figure 2.7: Parameters of end-cap modules in SCT [21]

The Atlas micro-strip sensors are fabricated using p^+ implanted ≈20μm wide strips in high resistivity n^- substrate. There are 5 different types of forward silicon sensors: W12, W21, W22, W31, W32. All of them have 768 readout plus 2 edge strips. [21]

2.4 ITk in ATLAS Upgrade

In the centre of ITk detector, sensors are arranged in the cylinders around the beam axis, starting with 5 pixel layers followed by 2 short-strip layers of paired stereo modules then 2 long-strip layers of paired stereo modules. The forward regions will be covered by six strip disks.[23] The table 2.8 shows number of components for the ITk strip detector in barrel(top half) and end-cap (bottom half).

Barrel Layer:	Radius [mm]	# of staves	# of modules	# of hybrids	# of of ABCStar	# of channels	Area [m^2]
L0	405	28	784	1568	15680	4.01M	7.49
L1	562	40	1120	2240	22400	5.73M	10.7
L2	762	56	1568	1568	15680	4.01M	14.98
L3	1000	72	2016	2016	20160	5.16M	19.26
Total half barrel		196	5488	7392	73920	18.92M	52.43
Total barrel		392	10976	14784	147840	37.85M	104.86
End-cap Disk:	**z-pos. [mm]**	**# of petals**	**# of modules**	**# of hybrids**	**# of of ABCStar**	**# of channels**	**Area [m^2]**
D0	1512	32	576	832	6336	1.62M	5.03
D1	1702	32	576	832	6336	1.62M	5.03
D2	1952	32	576	832	6336	1.62M	5.03
D3	2252	32	576	832	6336	1.62M	5.03
D4	2602	32	576	832	6336	1.62M	5.03
D5	3000	32	576	832	6336	1.62M	5.03
Total one EC		192	3456	4992	43008	11.01M	30.2
Total ECs		384	6912	9984	86016	22.02M	60.4
Total		**776**	**17888**	**24768**	**233856**	**59.87M**	**165.25**

Figure 2.8: Number of components for ITk Strip Detector [23]

2.4.1 Barrel modules

ITk with its outer radii will include strip modules consisting of short strips in the two inner barrel layers and long strips in the two outer barrel layers. Layout can be seen on figure 1.7. These modules in barrel region will be organized in staves, each with 13 modules per side. More information will be given in chapter 3.2. Mentioned staves are shown on figure 2.9

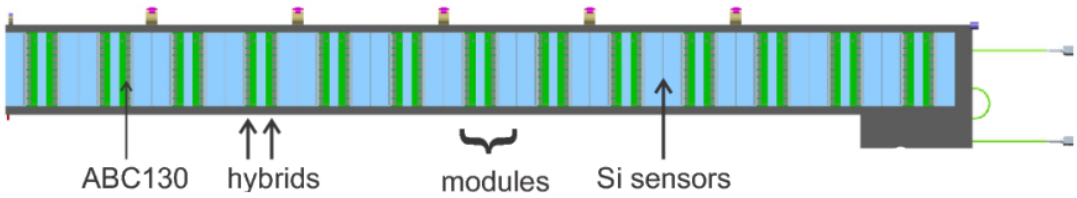

Figure 2.9: ITk barrel modules organized in staves [28]

2.4.2 End-cap modules

The inner detector, soon to be upgraded to ITk, consisted of both barrel and end-cap modules to minimize material seen by traversing particles as a function of polar angles. Due to the complex geometry of the end-cap, six different sensor designs are needed to cover petal surface. Each face of a petal has 9 sensors arranged in rings named R0-R5 from inner to outer radius. R0, R1 and R2 have one sensor per petal face and the outer three have two identical sensors per face.

Sensor layout is designed to minimize dead space. The chosen shape of all end-cap sensors so called "Stereo Annulus"(inner and outer edges are concentric arcs of circles, other two sides are straight, but do not point to the centre of the wheel). Finished end-cap structure consists of 6 disks on which the petals are mounted.[7] Design is shown on figure 2.10 with the supporting tube in the middle providing space for ITk pixel detector.

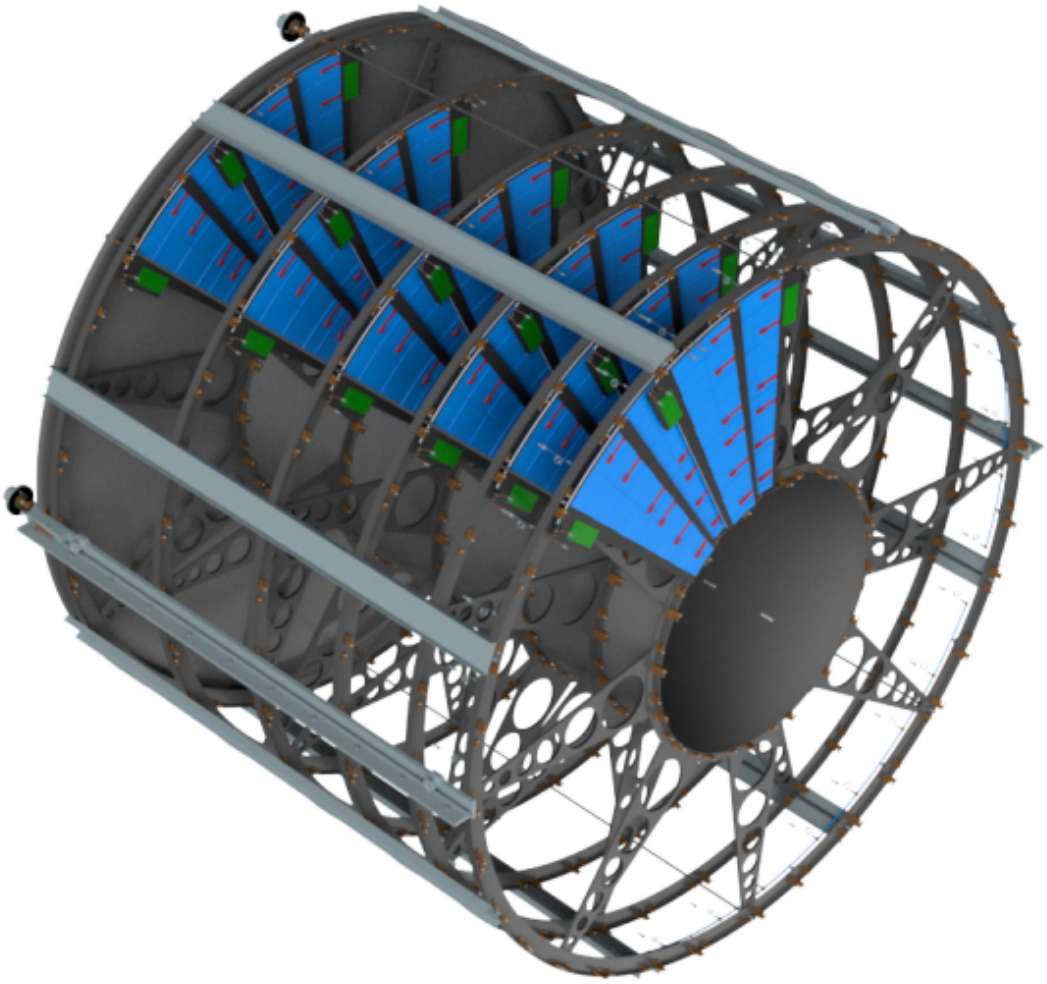

Figure 2.10: Global structure of the end-cap in a petalet structure [23]

The figure 2.11 shows computer generated image of an end-cap petal.

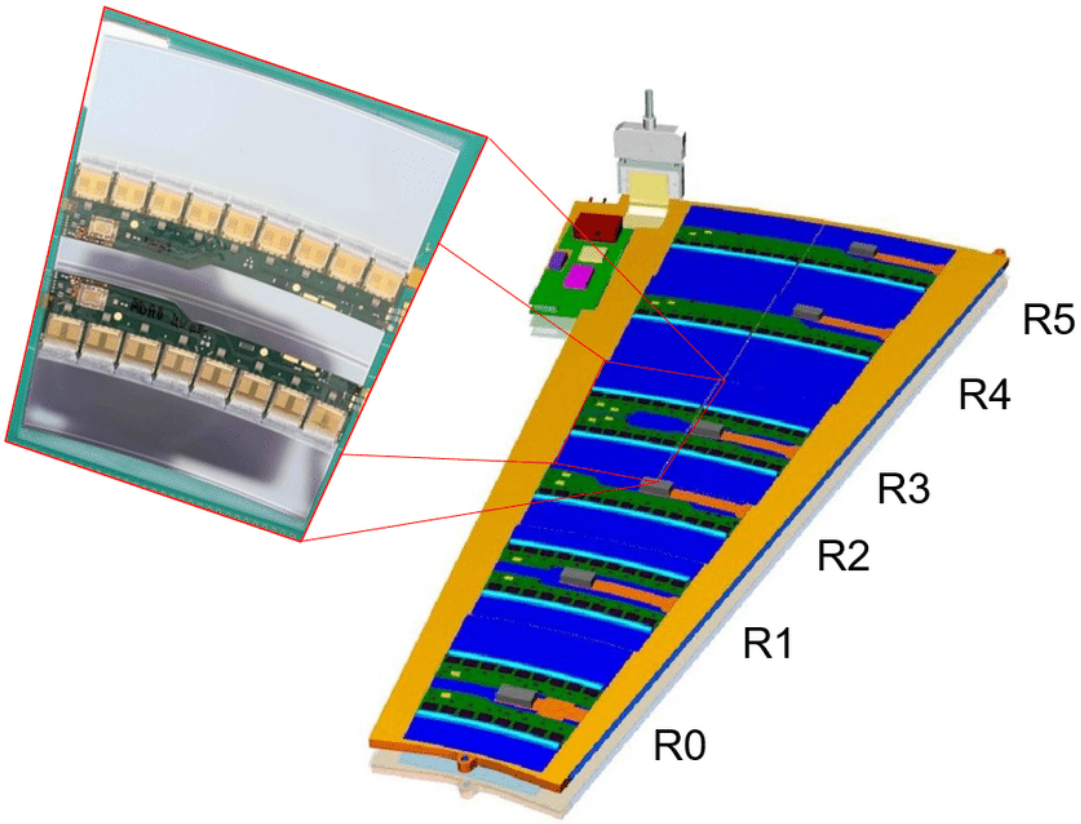

Figure 2.11: Global structure of the end-cap modules in ATLAS Upgrade [22]

3. Readout system in ATLAS Upgrade

The detector readout can be distinguished into two groups. The analog readout, providing us with the information about amplitude of signal. On the other hand we have binary readout providing us with only logical value, whether signal surpassed present threshold. This type of readout is used in Inner detector for tracking the particle, where the information about amplitude is not needed. Let us take a closer look at readout system in ATLAS Upgrade.

3.1 Binary readout

Binary readout provides us only with the information whether signal surpassed present threshold. This type of readout is used in Inner detector for tracking the particle where the selection of events is necessary. This readout method is chosen where the information of amplitude of signal is not needed. The reason of this choice is high number of collision observed by ATLAS, as logical information require less memory than amplitude. Selection of event is carried out by trigger system which functions on the principle of threshold. As particle crosses through detector it creates an impulse which is then sent to further examination if its magnitude passes certain value, in our case 1fC. The determination of this threshold is a crucial part of calibration of the device as we don't want to detect noise or uninteresting events, nor lose interesting events due to high threshold.

3.1.1 Trigger system

As an example of trigger system, we can discuss trigger system used in ATLAS. There the trigger system works on three level basis:

- Level 1
- Level 2
- Event Filter(EF)

LVL1 receives data at the full LHC bunch-crossing rate of 40 MHz . The output rate is limited by capabilities of the front-end system 75-100 kHz. Secondly, LVL2 and EF further reduce rate by the factor of 1000 where LVL2 provides reduction factor of 100 so the input to the EF is about 1 kHz. The figure 3.1 shows the three levels of the ATLAS trigger rates and processing time.

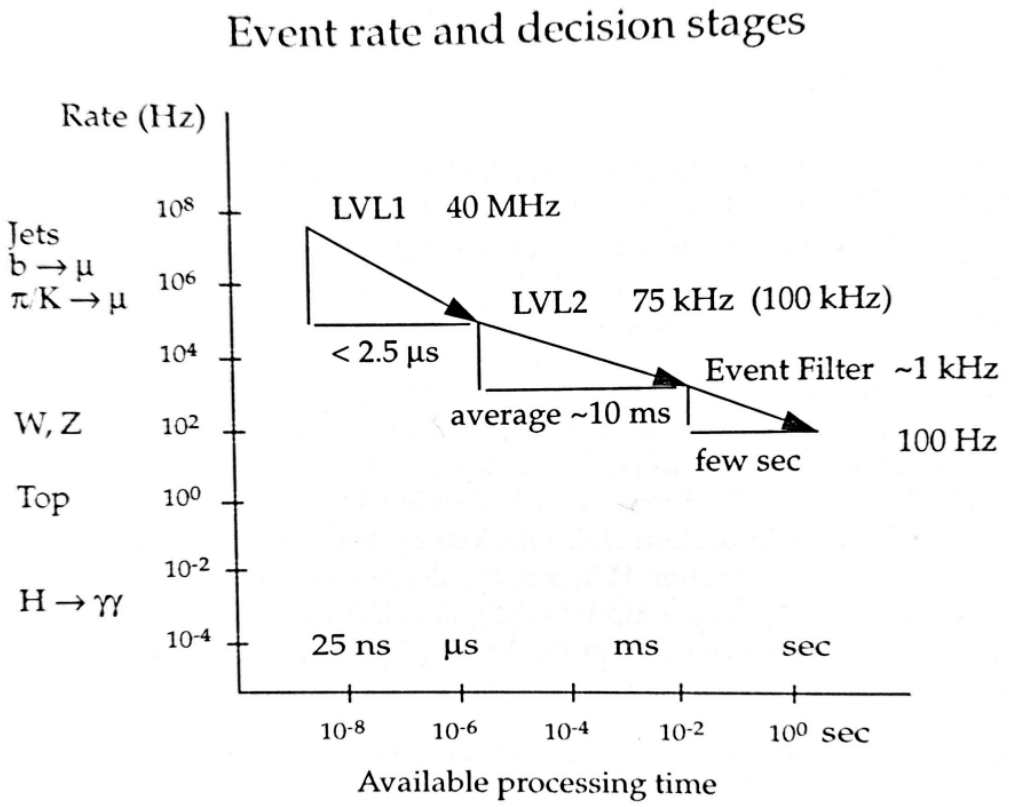

Figure 3.1: ATLAS Trigger rates and processing time [7]

Level 1

Level 1 - identifies the basic signatures of interesting physics. Its decision is based on multiplicities for various momentum thresholds. LVL1 algorithms are executed by custom electronics, the decision time of approximately 2μs also includes the transmission of signals. During the time of processing in LVL1, data from all detector system are held in pipeline memories. Upon acceptance of event, the data are read out, formatted and calibrated before being stored in readout buffers (ROBs), prepared for the use by LVL2 and EF.[7]

Level 2

The next stage, Level 2 trigger, is largely based on the use of regions of interest (ROIs). A small amount of information, corresponding to each object identified at LVL1, is passed to LVL2 for each event accepted by LVL1. For local objects the provided information is position and momentum threshold range. The regions flaged by ROIs are being further analysed by higher-level triggers. LVL2 processors, using more detailed detector data around the position indicated by the ROI, perform evaluation of the objects identified at LVL1. Thus, reducing event data needed to be moved from ROBs to the processors, thereby lower the required bandwidth and processing power of LVL2.[7]

Event Filter

The final selection step is being performed by EF. In this stage the full event is collected from the ROBs and then the EF operates on the complete event using full range of the detector. Processing time of order of seconds. A reconstruction is possible using several algorithms, though calibration and alignments constant are not final yet. Some of the possible algorithms used in this stage are: vertex reconstruction, track fitting, bremsstrahlung recovery for electrons. There are also some operation that require larger ROIs than those used in LVL2 such as γ conversion searches. The EF processing chain is guided by results of LVL1 and LVL2 in a similiar manner as LVL1 guides LVL2. Finally, the EF completes the classification of the events, catalogues discovery-type events, and stores them in database.[7] The figure 3.2 shows the three levels of the ATLAS trigger rates and processing time.

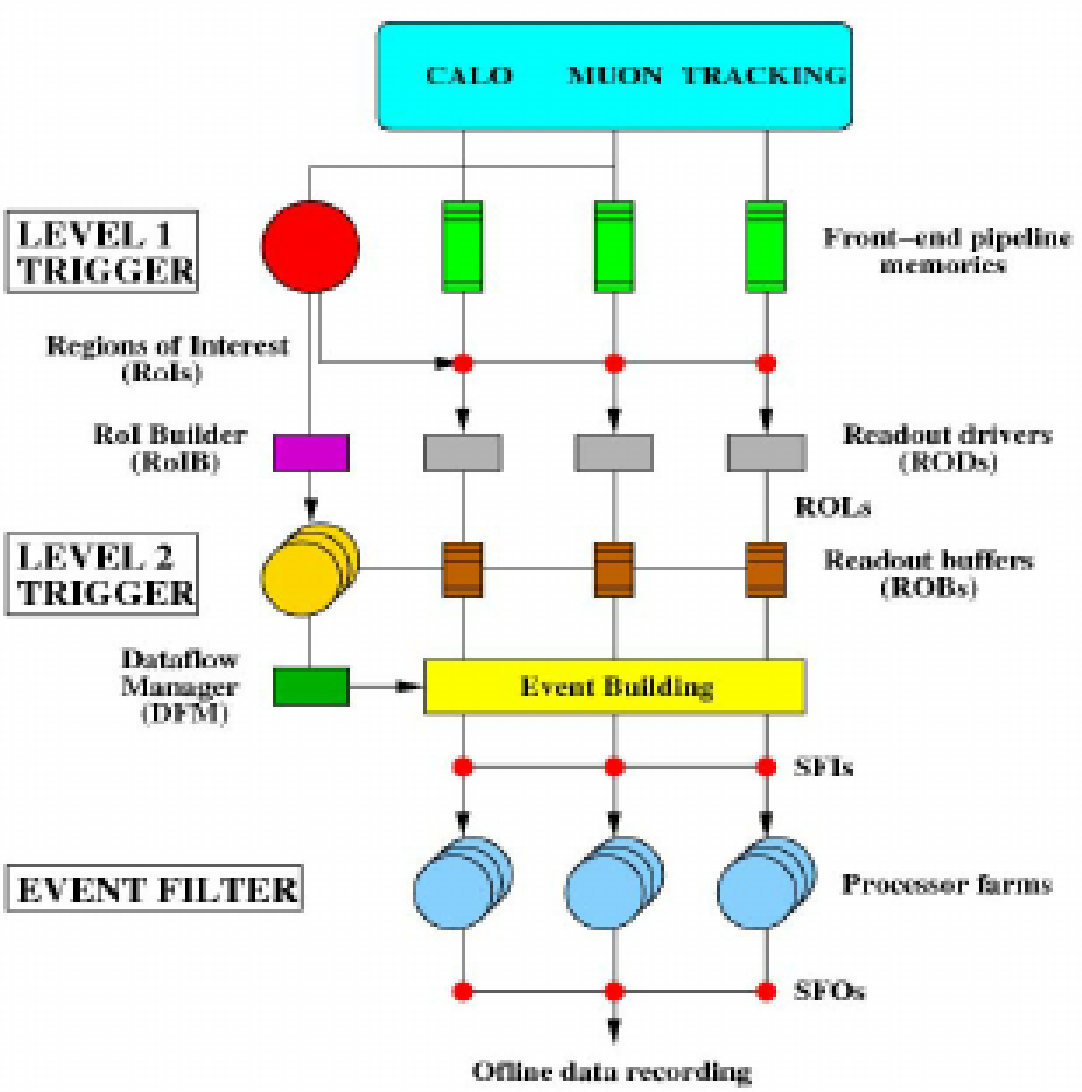

Figure 3.2: Layout of ATLAS Trigger levels [7]

3.2 Readout Hardware

Each module contains two ASICs(Application Specific Integrated Circuits) used for the readout of data. Digitization and cluster of data is done by ATLAS Binary Chips (ABCStars). Hybrid consists of 6 to 11 ABCStars and Hybrid Controller Chip (HCCStar), which purpose is to dispatch received trigger commands into attached ABCStar. New star configuration directly connects ABCStar and HCC-Star without bottleneck in data transfer apart from its predecessors. The figure 3.3 shows module from barrel region.

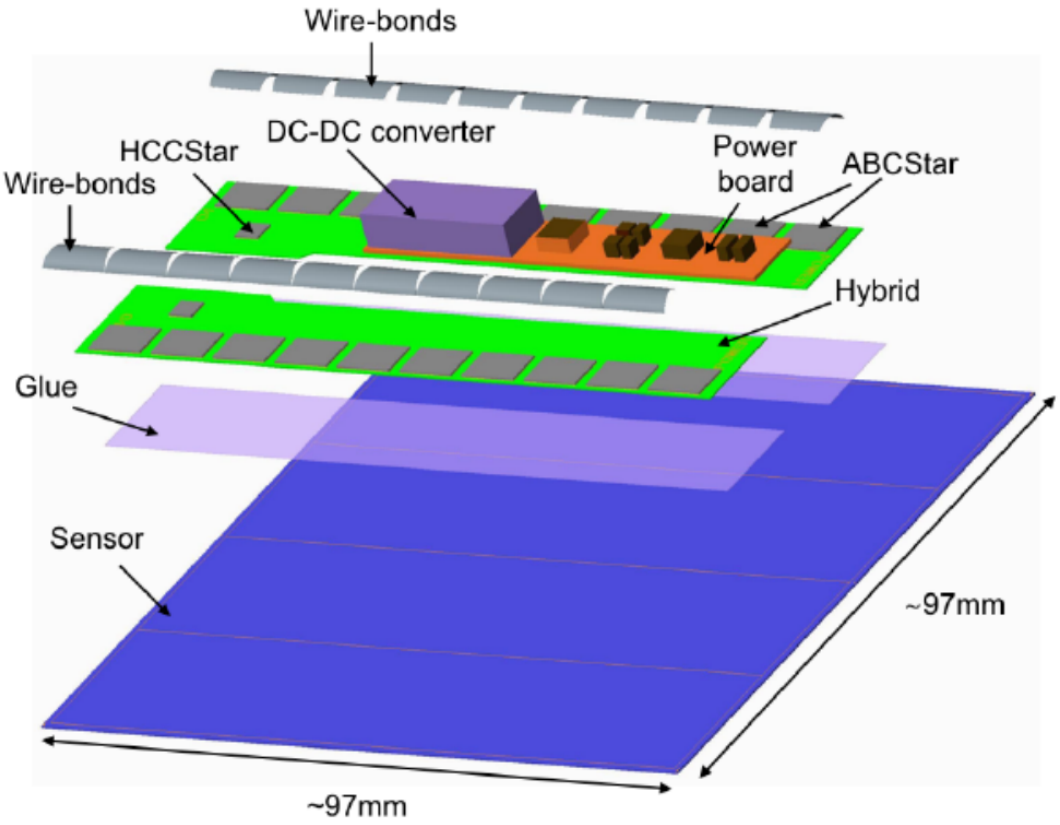

Figure 3.3: Diagram of ITk Strip [24]

ABC130

The ABC130 is a chip used in barrel module with 130 nm construction technology. It is the second generation of the ATLAS strips readout family. The chip must be ready to provide all the necessary functions for processing signal from 256 strips of silicon detector employing the binary readout architecture. The die with a size of 6.8 x 7.9 mm^2 is oriented orthogonaly to the direction of the sensor strips with the wide side. The figure 3.4 shows simplified diagram of the chip with the main functional block being:

- Front-end
- Command decoder

- Input register
- Pipeline
- Event buffer
- Readout logic
- Threshold and calibration control
- Power regulation

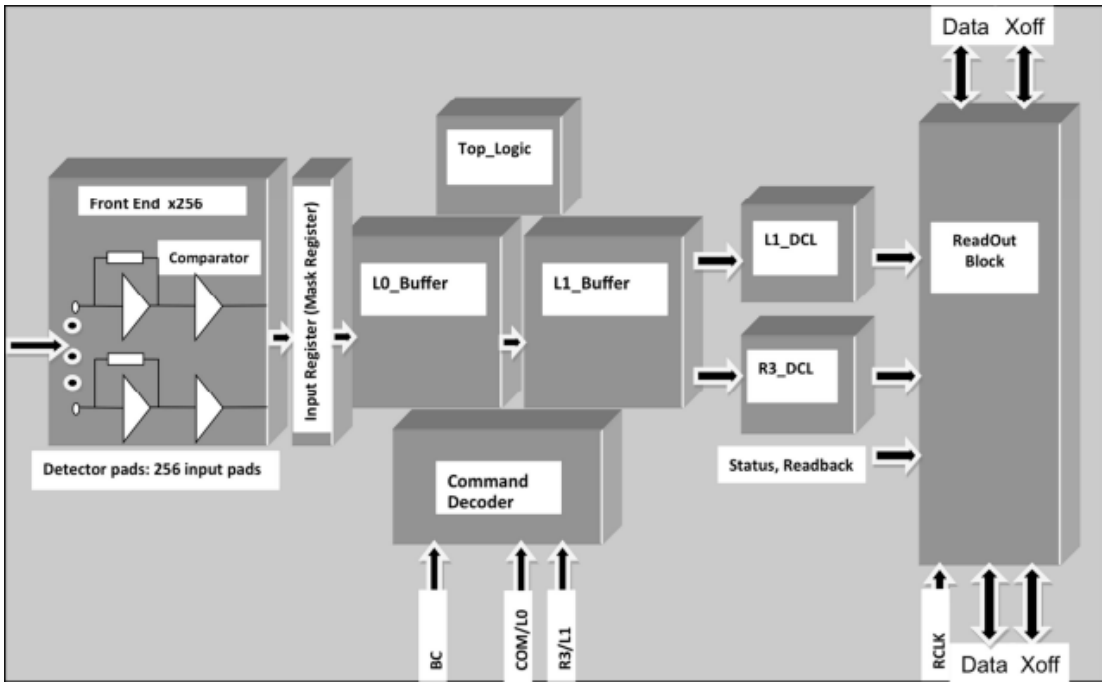

Figure 3.4: Chip ABC130 diagram [7]

Apart from formerly used chips ABCN-25, ABC130 allows multi-trigger flow possible by the doubling of the number of readout channels per chip.[25] [26] The front-end input pads are arranged in configuration of staggered rows of 64 pads each bonded with a wire to the AC sensor pads. These pads are arranged so that one ASIC amplifier channels can be connected to two rows of sensor strips, these connections are interleaved allowing cross-checking. The figure 3.5 depicts the layout of pads in ABC130.

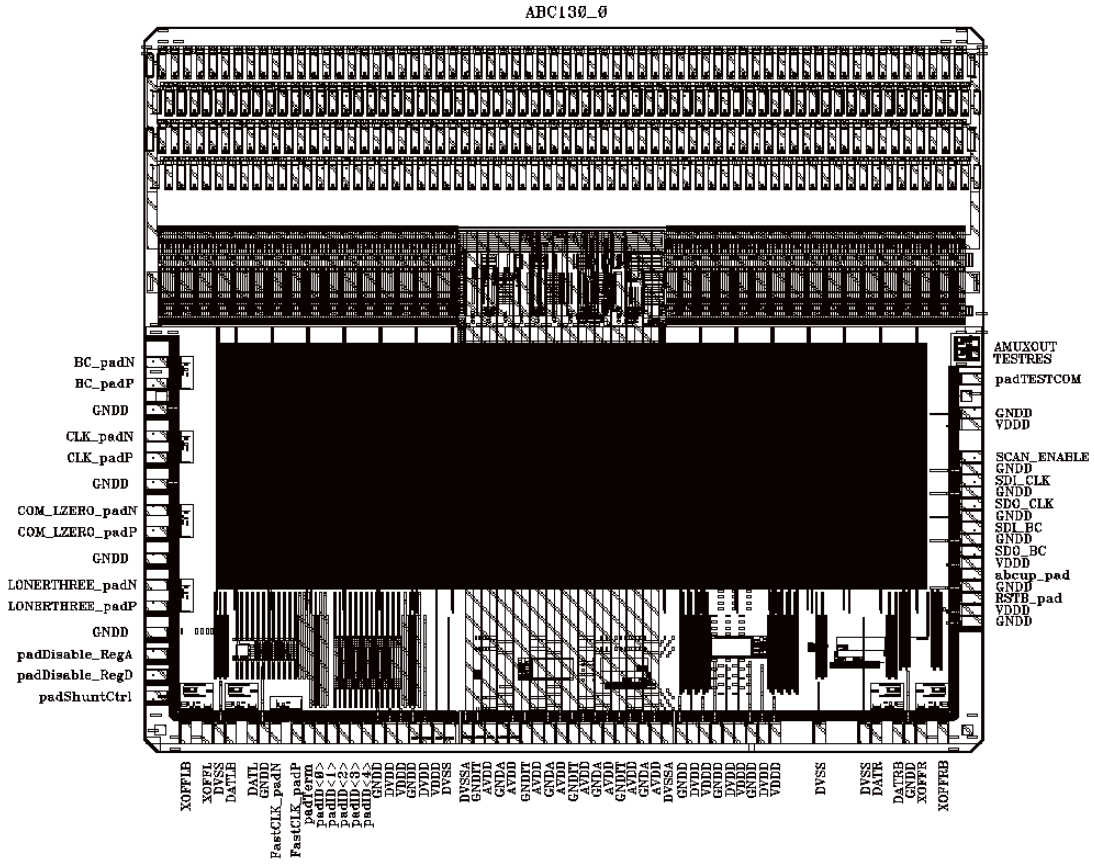

Figure 3.5: ABC130, Layout of pads [26]

The architecture has 3 main stages:

- Inputs are sampled from front-ends on every cycle of BC (LHC Bunch Crossing, 1 BC=25 ns) and put into pipeline (L0 buffer) allowing external process(L0 trigger) to chose which crossing to read out(up to 6 μs).
- After the acceptance of event the data arrives at the ABC130 and the appropriate data is copied to the L1 buffer.
- Afterwards the final readout command(R3 or L1A) can be received up to 512 μs later.

The regional Readout request (R3) is acted on by small proportion of modules, selectable at the HCC-level, based on the position of the module in detector, providing fast readout of data which can provide input for L1 trigger system. On the contrary the purpose of L1A is to read out full information for the required BC.

The figure 3.6 show physical ABC130 barrel modules.

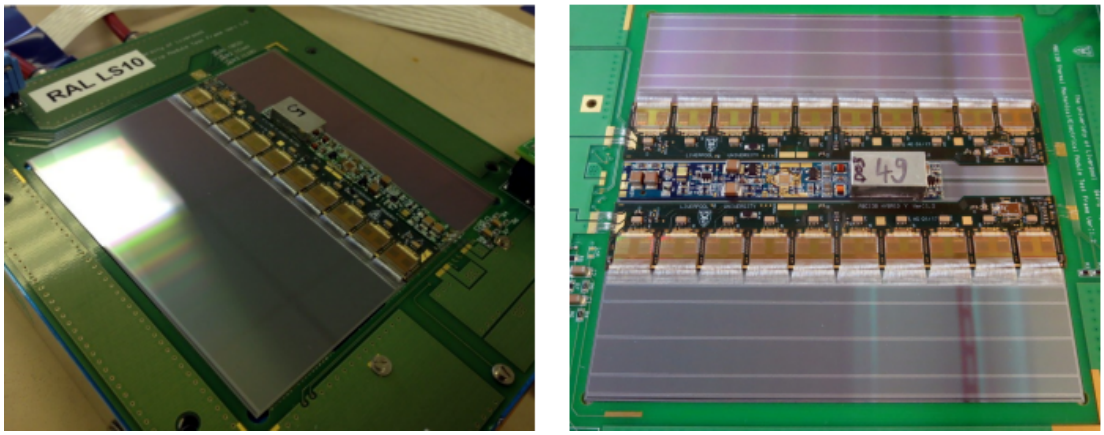

Figure 3.6: ABC130 long-strip(left), short-strip barel modules on a test frame [26]

HCC130

. The HCC130 (Hybrid Chip Controller), ASIC with 4.7 x 2.96mm^2 and 99 pads was constructed to provide interface between the hybrid-mounted front-end ABC130 and the off detector electronics. HCC130 receives bunch crossing clock of 40MHz and two protocol control signals. All types of data sent from modules are transmitted to the GBTx by HCC130 at 160 to 320 Mbps. There are several control signals used by HCC130 [26]:

- L0_COM beam trigger that stores the ABC130 pipeline delayed data into data buffer from which they are requested for readout.
- Priority based variable length command (COM) is a second logical channel of L0_COM signal, that controls operation modes in HCC130 and ABC130 and initiates data requests from internal registers.
- R3s_L1 provides two triggers used for requesting readout data from ABC130. The L1 is broadcast to the ABC130s where it requests readout data from one of the 256 memory locations in the L1 buffer. In addition to the the R3 part, containing 14 bits, propagates signal only to HCC130 with matching addresses, if the addresses match the previously masked bits from ABC130 are broadcast into ABC130s.

Upgrade of chips

The LHC is scheduled to undergo a upgrade where ABC130 chips will be replaced by ABCStar chips as well as HCC130 will be replaced by HCCStar as they could not support the latest trigger requirements. These chips are being currently tested since January 2022. Said upgrade is supposed to prepare detector structure for higher luminosity by improved radiation resistance and finer granular detector structure as the density of events will increase. The fundamental change was the process of the data transfer. Serial transfer of data to HCC was changed to

direct communication from all ABCs to the new HCCStar, removing the bandwidth bottleneck in data transfer. The figure 3.7 shows schematics of different connections of ABCs and HCCs.

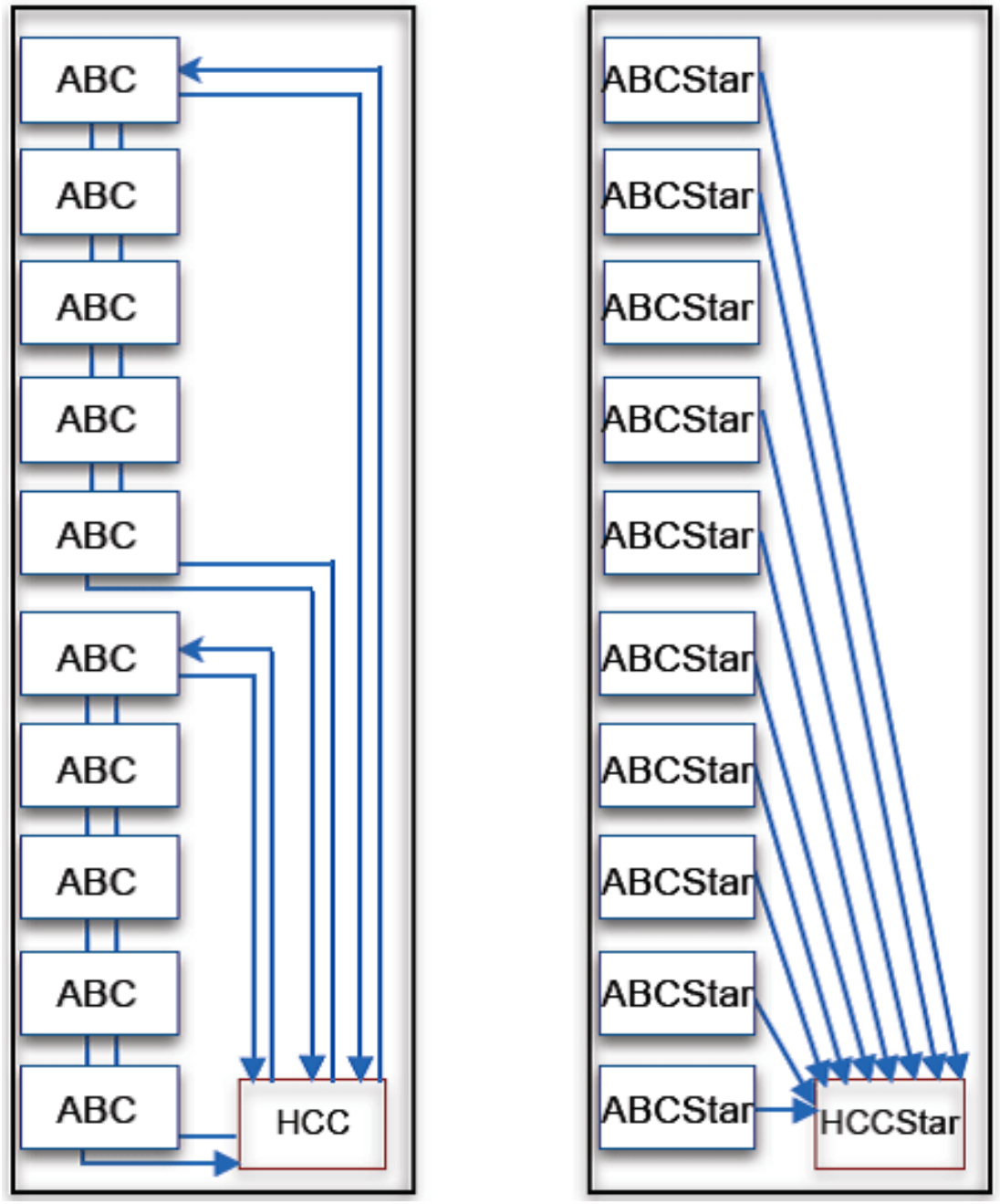

Figure 3.7: Connections of different layouts: 130(left), Star(right) [27]

3.3 Readout Software

The software used for the readout is called ITSDAQ (ATLAS ITk Strips Data Acquisition) compatible with Windows and Linux systems, its predecessor was called SCTDAQ, developed for testing of SCT modules. The ITSDAQ, working in the environment of ROOT, allows setting of various chip parameters as well

as scan variable characteristics for the measurement. There are three identifying numbers for each measurement : run, scan and burst number. Furthermore, upon running the program three windows appear[28]:

- Burst data - used for manual setting of scan parameters, and shows data packets from bonded channels of the sensor.
- Scan data - shows final results of each scan.
- Root command window

The figure 3.8 shows the appearance of windows during measurement run on Linux operating system.

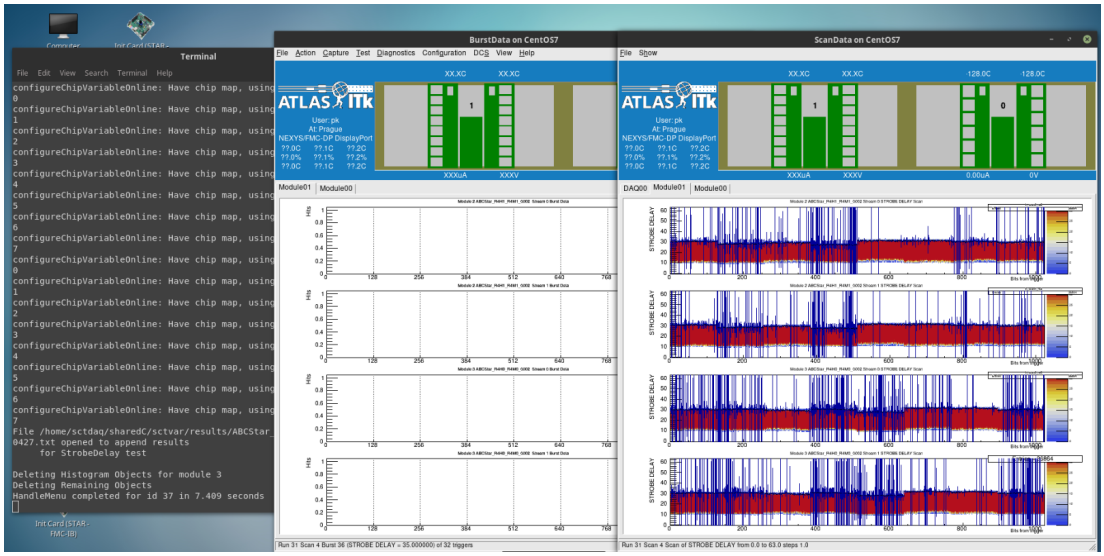

Figure 3.8: Windows showing simultaneous measurement of pedestal scan on STAR R2 and STAR R4 module. Provided by Mgr. Martin Sýkora.

Depending on type the input/output of ITSDAQ is stored in sctvar/ directory. Its sub-directories are used to save important results from scans or hold essential macros to run scans. These sub-directories are [28]:

- config/ - contains all the files used to configure modules for testing and scan itself
- macros/ - scripts for running tests
- data/ - raw data from tests(eg.channel hits)
- results/ - calibration results, and the results of tests from module characterization. Results from each channel are stored in text files.
- ps/ - visual results, such as plots

Macros

β-source tests - we usually distinguish between 2 types of macros and those are: data acquisition macros and data analysis macros used, for instance, for analyzing the distribution of simultaneously hit strips or fitting and creating S-curve (mentioned later) by two different methods and converting DAC(DAQ counts or internal variable) to mV a fC. If we try to briefly describe function of a data acquisition macro we could divide it several parts:

- Configuration - firstly, macro sets optimal initial parameters of the scan
- Data acquisition - after proper configuration scan itself is launched, resulting in data acquisition. Test itself consists of gathering of threshold scans for different injected charges.
- Data analysis - macros specifically used for data analysis are launched with the parameters and data from previous scan. The output can be in various variables(DAC, mV, fC), but can be converted to one another using results from three point gain scan and response curve.
- Ploting - lastly, plots of results are generated.

Laser tests - macros for Laser tests consist of:

- Configuration - firstly, initialization of module takes place setting it in optimal state awaiting previously defined trigger(internal/external). Apart from β-source macros configuration of laser additionally consists of: setting of power and timing of the laser pulses (for example using generator Agilent81110A), initialization of motors used for setting the exact position, and sometimes setting intensity of the pulse.
- Data acquisition - data acquisition runs analogously as β-source threshold scans, with the difference in changing the position of laser impact and pulse intensity.
- Data analysis - just as in β-source tests macros for data analysis are launched and plots are generated from results of Vt50 (mean).

3.3.1 Calibration and detector characterization

Before the sensor test the check of basic properties of the module is needed. The calibration is usually done after each configuration change in order to reach proper timing and response variability. These basic calibration scans are part of ITSDAQ macros and are executable from burst data panel as well as from ROOT session command line.[28]

Threshold Scan

This calibration is done on the principle of injection of constant through the calibration circuit and varying threshold discriminator from zero to its maximum. The increasing threshold causes gradual signal disappearance for each channel.

For each threshold level several charge injections are performed. Plotting the average hit rate versus threshold gives a S-curve plot. S-curve, also known as Skewed complementary error function, is approximation of Gauss-convoluted Landau distribution measured in threshold scan. We use it to fit measured data. Signal decrements are represented by efficiency loss, which is defined as a number of triggers with signal divided by total number of triggers. Vt50 is the value with a 50% hit rate corresponding to the median of the injected charge. Qt50 is same value but in fC.[7] The figure 3.9 shows average hit rate versus threshold for a ABC130 at 1.51 fC injected charge.

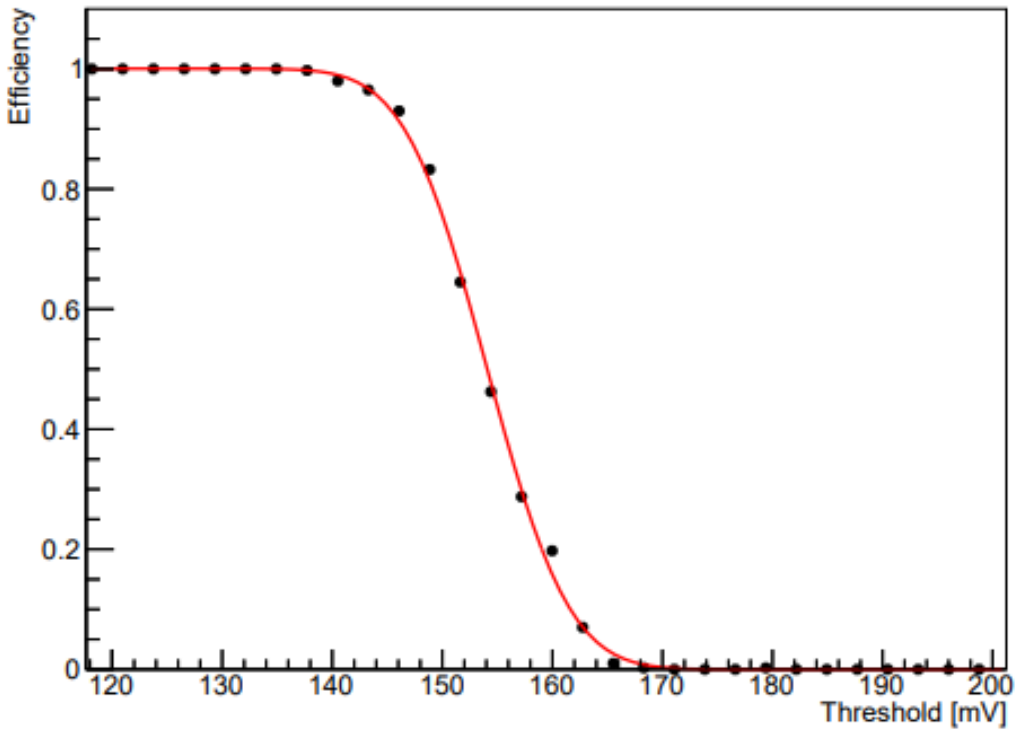

Figure 3.9: Average hit rate versus threshold for a ABC130 at 1.51 fC injected charge (S-curve) [7]

Strobe Delay

In the newest version, also known as pedestal scan, is a scan whose purpose is to set the timing (delay) of an injected calibration pulse with respect to the arrival time of the command to actually issue that pulse(Level 1 Accept trigger). This ensures that the discriminators will be synchronous with the calibration signal, preventing efficiency losses. This test should be executed before each measurement. Figure 3.10 shows result of strobe delay test.

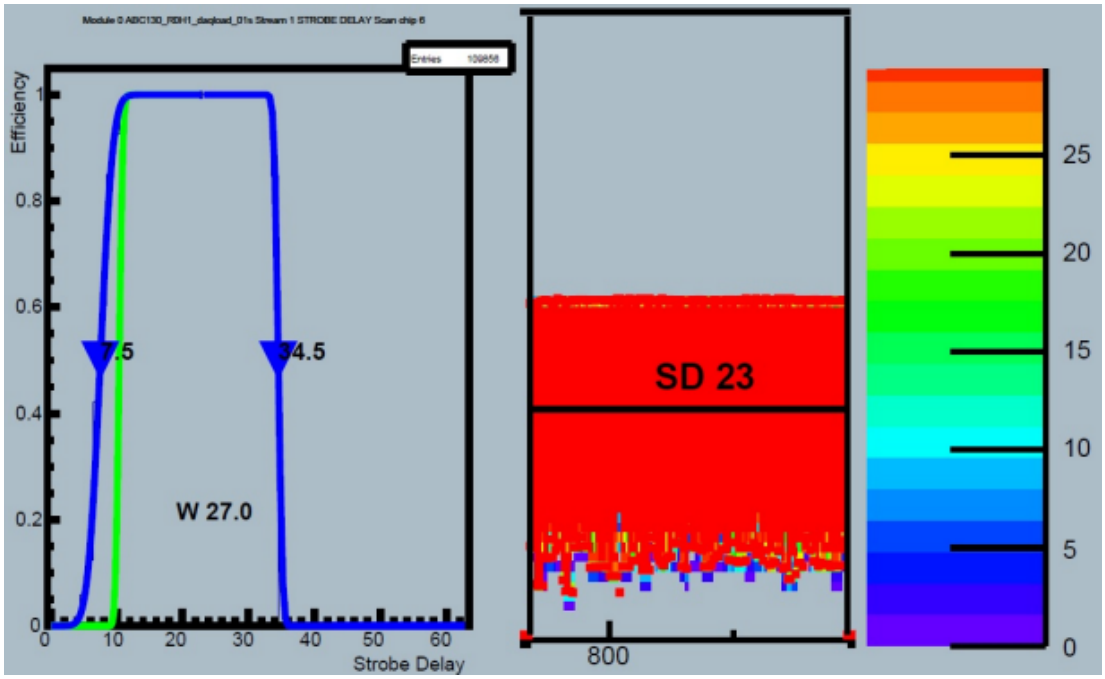

Figure 3.10: Result of strobe delay test [28]

Three point gain

The last step in conversion of mV to fC the knowledge of response curve is needed. For lower charge values we can approximate response curve by three point gain test, thus saving computing time. The threshold scans are performed for three different injection charges, typically 0.5fC, 1fC and 1.5fC. The response curve is then linearly fitted as a function of injected charge to obtain values of discriminator offset (pedestal) (mV at 0fC) and the channel gain (slope of the curve).

$$Vt50[mV] = gain[mV/fC] \times Qt50[fC] + offset[mV] \tag{3.1}$$

Resulting offset (pedestal used to balance out individual channels) and gain (amplification done by electronics) are evaluated for all readout channels in single readout chip.

Response Curve

Extended test of three point gain is performed especially for higher charges, as relation between internal units may not be linear for higher charges. This test is based not on three but on ten threshold scans up to 6fC. For each injected charge the Vt50 point is measured and then plotted as a function of the charge.[28] [7] The figure 3.11 shows comparison of 3PG and RC calibration scans

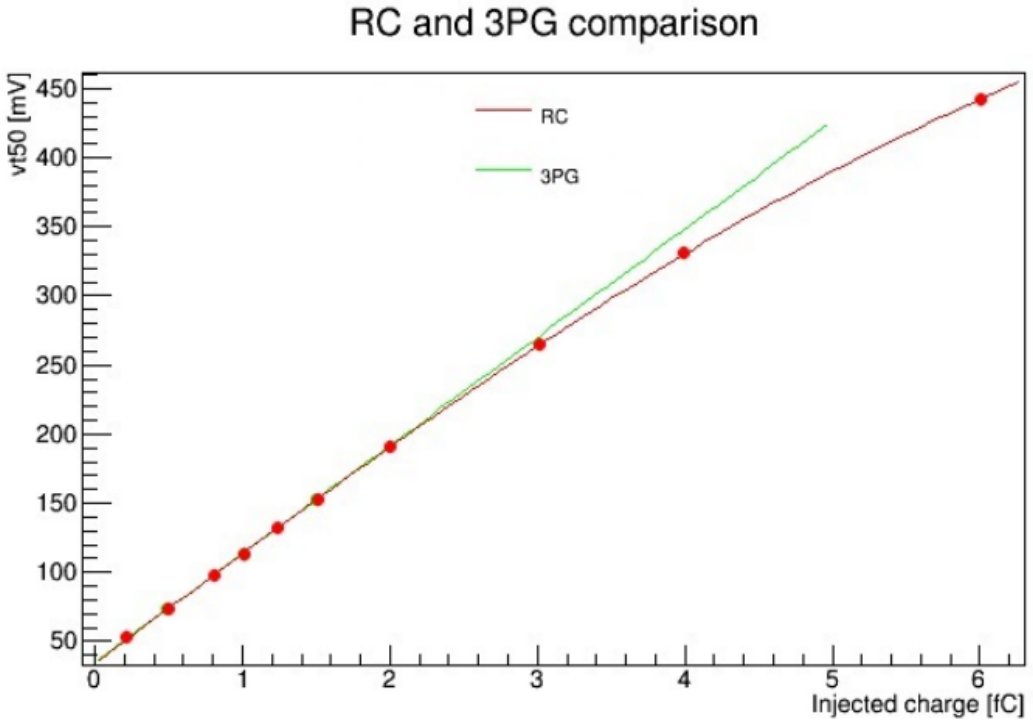

Figure 3.11: Comparison of 3PG and RC calibration scans [28]

Noise Occupancy

The noise occupancy(NO) is a critical parameter for binary readout. The scan measures noise occupancy as a function of threshold. NO is defined as number of hits for the equivalent threshold of 1fC. The required channel noise occupancy for ITk Strip detector is less than $1x10^{-3}$, giving us a efficiency greater than 99%. Figure 3.12 shows example of plot of signal efficiency compared to the noise occupancy.

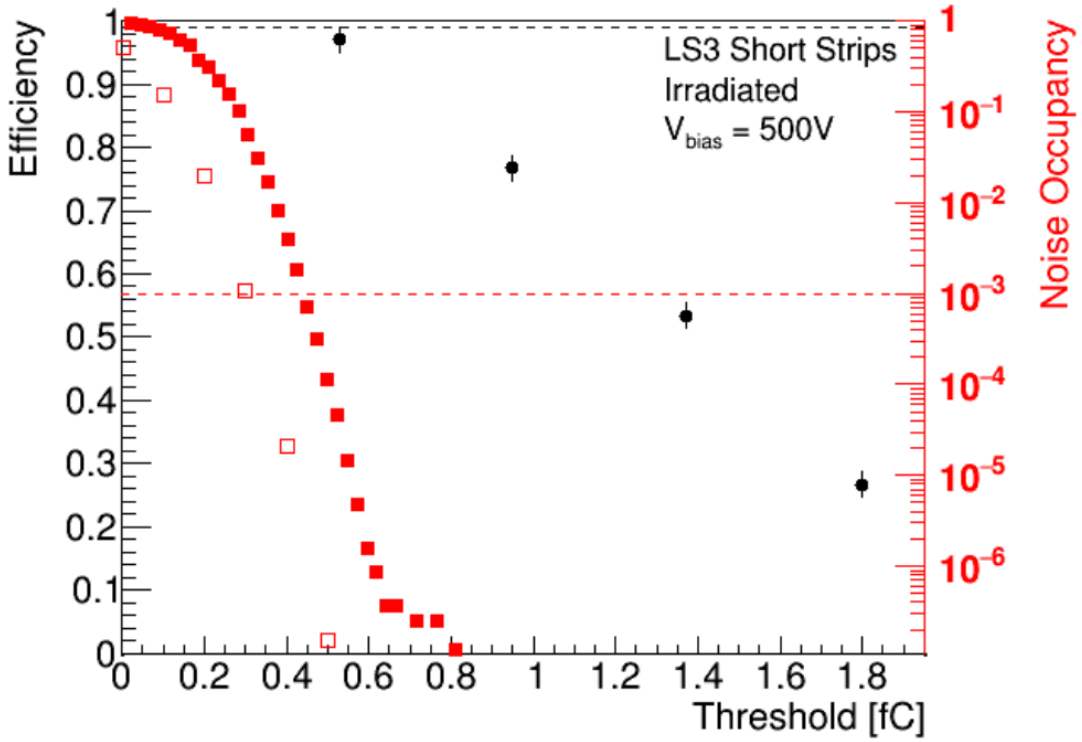

Figure 3.12: Example of plot of signal efficiency (black dots) compared to the noise occupancy at different thresholds for the ABC130 (red squares) and new front-end (open squares) [23]

Noise is ever present disturbance of every electronic signal. Using ITSDAQ software (mentioned earlier 3.3) we are able to evaluate this disturbance. As a one of the results from three point gain calibration comes information about noise. Noise is defined by two values: input noise (innse), defined an injected charge at the input that would simulate the same signal at the output as obtained from the noise, and the output noise(outnse), corresponding to dispersion σ factor from 3PG, related by[28] [29] :

$$innse[fC] = \frac{outnse[mV]}{gain[mV/fC]} \tag{3.2}$$

Figure 3.13 depicts channel input noise for 128 channels.

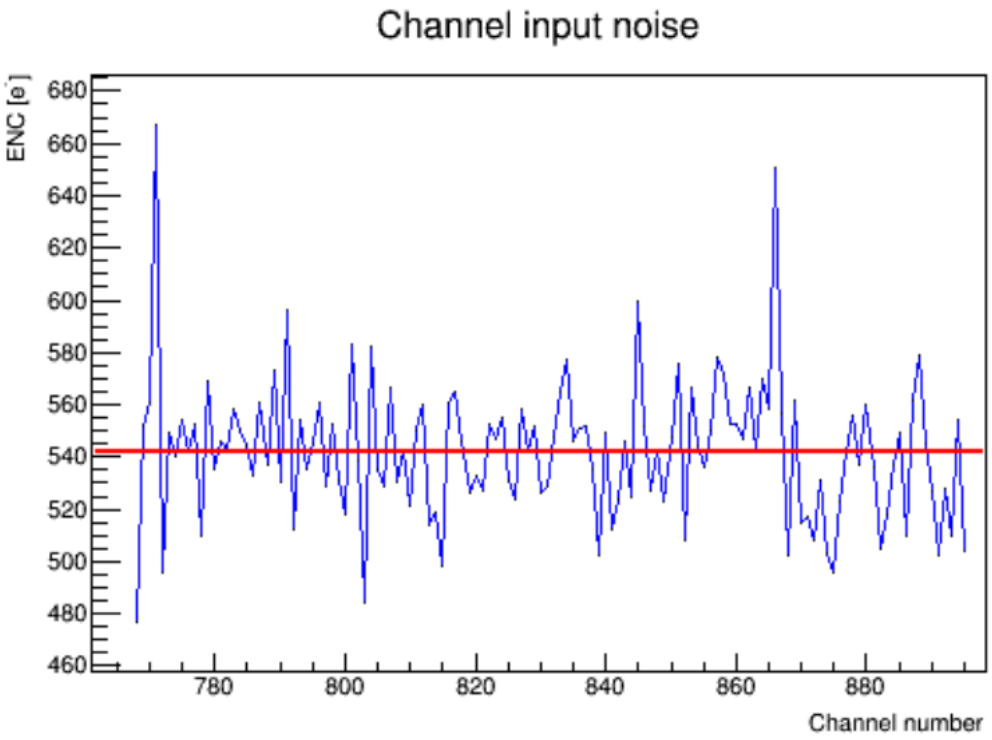

Figure 3.13: Value of input noise for each channel at default setting of FE(front-end) parameters [28]

This procedure finally leads to obtaining parameter know as **Signal-to-Noise Ratio** (SNR). SNR is the defining parameter of electronics and can be calculated with the knowledge of median charge values from threshold scan as[29]:

$$SNR = \frac{Vt50[fC]}{innse[fC]} \tag{3.3}$$

3.4 Preparation for termocycling tests

At the time of writing this thesis, the new termocycling tests on modules R2 and R4 are being conducted at Prague laboratories of Institute of Particle and Nuclear Physics. The tests consist of measuring the outputs of 4 modules, some of which have dummy sensors, during the 16 hours temperature cycle ranging from -40°C to 40°C. Tests are conducted to determine the durability of electronics and sensor itself and also to find out the ability to withstand different conditions. Modules are located inside thermally isolated box. Temperature is controlled by heater/cooler and not by nitrogen. Environment of the test must be properly prepared and monitored as frozen water from natural humidity could damage electronics. The output from individual modules is then carried to multi-module readout card and subsequently to the ATLYS readout card resulting in faster processing of data as we can gather data from 4 different modules at once. Data are finally analyzed on connected computer setup with preprogrammed macros. The figure 3.14 shows mentioned box with connected modules two R2 modules on left and two R4 modules on right.

Figure 3.14: Temperature cycle setup in Prague laboratories

4. Special Tests

Upon finishing the manufacture of a detector there is a need for mandatory tests of its functionality and properties. These tests are intended to smooth out possible imperfections and finish up a fully functional device for an experiment. Part of testing is examination of the device in various conditions in order to determine the finest possible detecting performance test.[31]. Several methods are used for the testing, they usually vary by the source of signal:

- Laser test
- Test beam
- Source test

4.1 Laser test

In this method, a short-pulsed laser beam is used for the detector illumination. The light is lead through an optical fiber being prepared and focused on the detector. The preparation of beam consists of setting the polarity, amplitude and width of pulse. The advantage of this method is that we are able to focus the beam on specific location with the diameter of well focused beam being few μm. Another advantage of laser tests is that we are able to control the beam apart from β-source test where creation of particles is a thing of statistics, thus enabling us to prepare the timing of the configuration. One of the disadvantages of laser tests is the interference caused by protection layers of sensor that can result in amplifying generated charge up to double of its real value. Aside from difference in intensity of the pulse, laser tests can differ in used wavelengths of the pulse. The cheapest option would be red wavelength laser, but the downfall is weak tunneling ability in the sensor (only 10μm with width of sensor being 300μm). Therefore, frequently used wavelength is infrared being able to tunnel up to 4mm in sensor material. The basic scheme of optical head used is shown on figure 4.1.

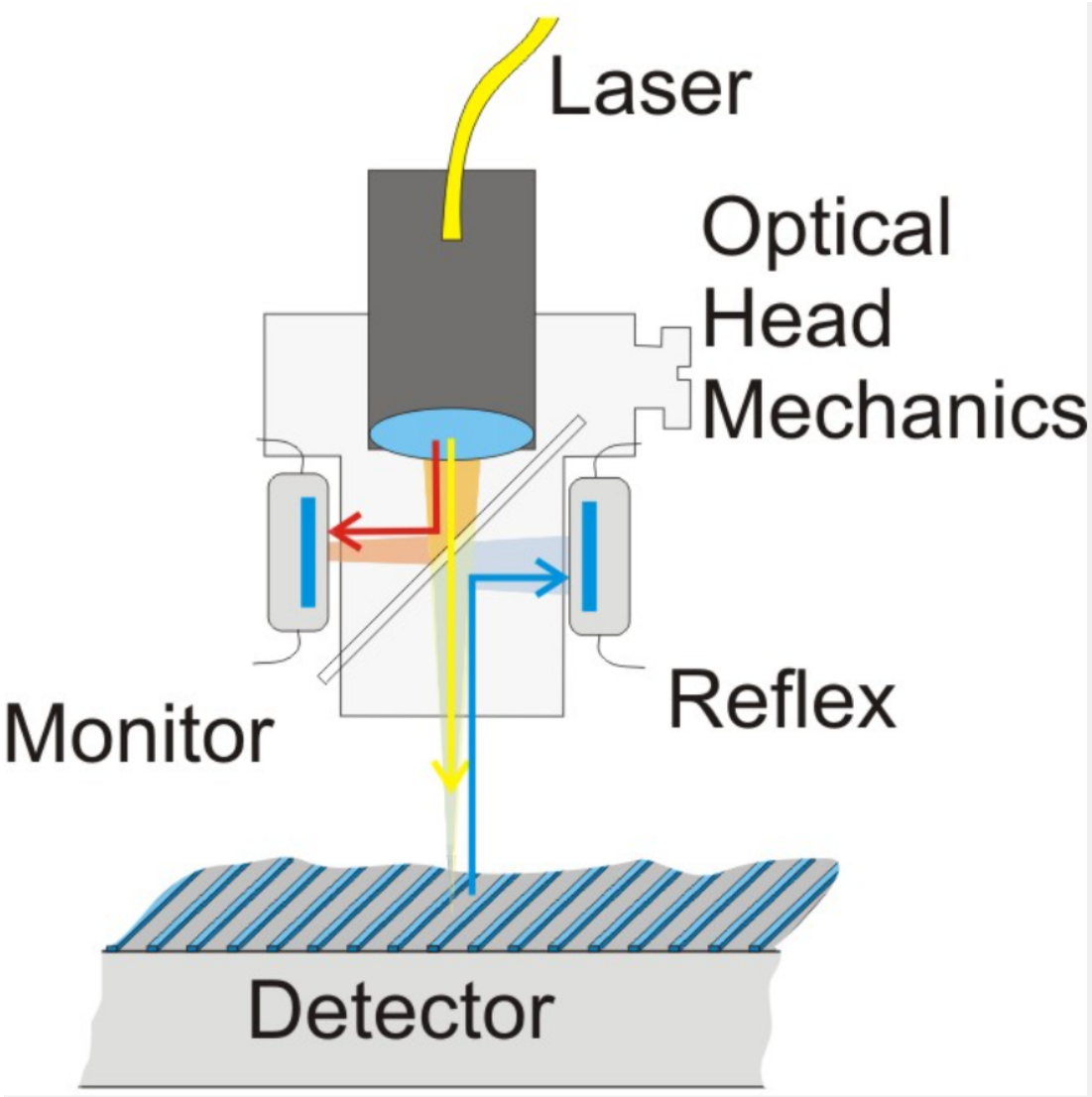

Figure 4.1: Configuration of Laser test [30]

4.1.1 Laser tests in Prague

The laboratory for laser tests in Prague is located in clean room. The environment of the room is monitored for temperature and humidity in order to prevent any damages. Furthermore, the said laser tests are performed in a heat isolated box with temperature regulation, as observations taught us that fluctuations of temperature in the box yield different results. The laser test setup is at the moment disassembled, as it will undergo upgrade. As a result of this we were not able to performed any laser tests at the time of writing this thesis. The figure 4.2 shows interior of box used for laser tests.

Figure 4.2: Interior for box prepared for laser tests

Figure 4.3 shows typical response of position scan over strips done on Hamamatsu detector with infrared 1055nm laser.

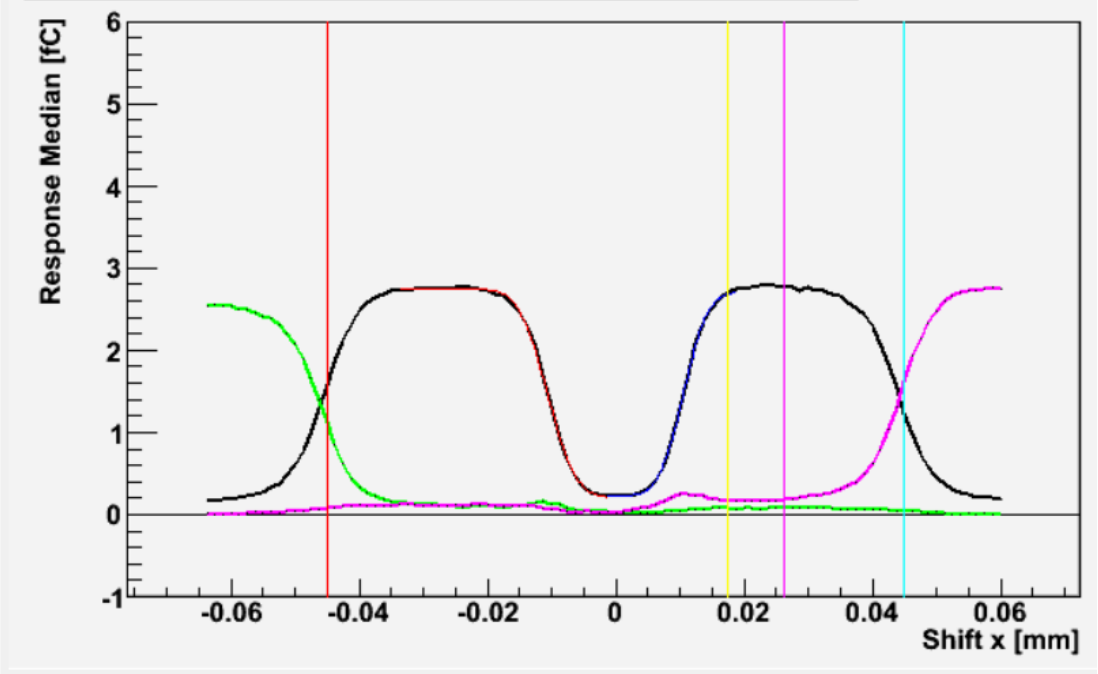

Figure 4.3: Laser test response of position scan over strips done on Hamamatsu detector, Prague 2006

[30]

4.2 Test Beam

Device under test (DUT) is placed between telescopes which play the role of reference detectors. These telescopes are there to estimate the position of particle before and after it passes through tested module. The comparison of measured positions on all detectors yields DUTs spatial resolution. Particles used in this method are: hadrons-mainly protons and pions(in Geneva), and electrons(in Hamburg). Scintilators are used for triggering the system. The main sources of uncertainty are the contribution of the multiple scattering and precession of individual telescope. Minimizing the amount of material can result in greater precision in lower energy beams. On the other hand with higher energy beams the scattering component decreases. One of the drawbacks of this method is cost, β-source tests are more available in this regard.[31]

4.3 β-source test

The radioactive decay is used in this method as a source of particles. The nuclei of unstable isotopes can undergo two different process, β^- decay and β^+ decay. In the case of β-source tests in Prague a isotope of Strontium ^{90}Sr is used which decays into Yttrium ^{90}Yr and finally to ^{90}Zr. The main objective of this test is to measure charge collection efficiency. The issue in this tests is the charge

deposition into the silicon as low-energy part does not have enough energy to pass through detector, resulting in deposition of entire energy into the silicon. The figure 4.4 shows setup for beta testing in Prague IPNP laboratory.

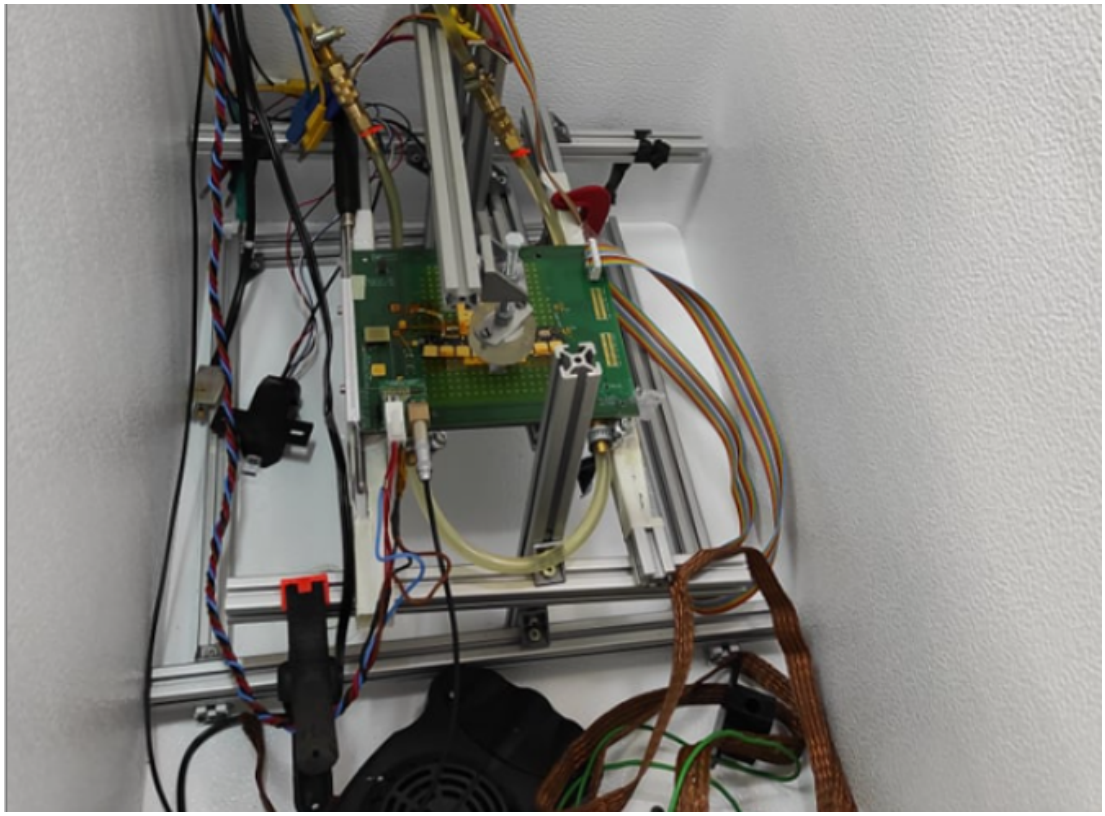

Figure 4.4: Beta source setup

Trigger scintilator signal shaping in β-source tests

In a process of testing we are provided by an output signal which needs to be analysed in order to obtain information. The signal output is usually short pulse with small amplitude. This output needs to be modified and processed for us to be able to analyze it. Modifying is done by series of electric circuits which schematics is shown on figure 4.5.

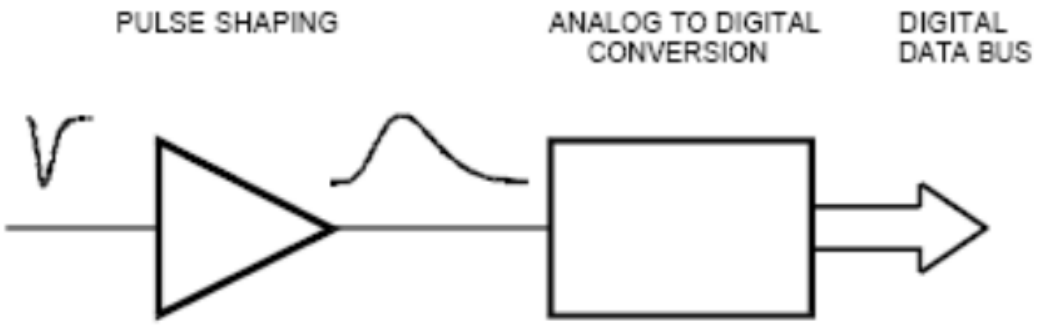

Figure 4.5: Schematics of signal processing [32]

We will discuss some of the parts responsible for signal shaping:

- **Preamplifier** - constructed closest to detector in order to minimize noise, which is proportional to the cable length. Transistors are most commonly used as a preamplifiers and their purpose it to convert weak electrical signal into strong enough output signal for further processing.
- **Pulse shaping circuit** - transforming fast steep pulse into broader one, allowing us easier amplitude measurement and to correct fluctuations caused by the noise. Broadening of the pulse minimizes noise, but on the other hand can cause effect called **pile-up** (piling up of pulses on one another), resulting in distortion of amplitudes. Figure 4.6 shows pulse shaping.

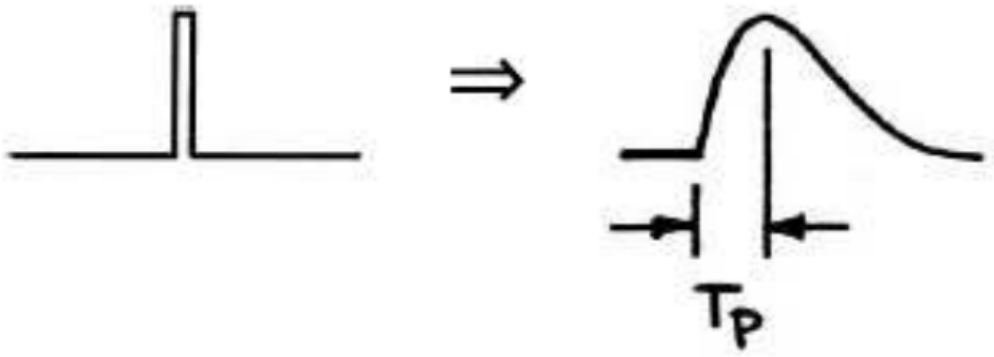

Figure 4.6: Pulse shaping [32]

- **Digitization** - we often need to digitize output signal. In case of analog signal this achieved by analog to digital converter (ADC). ADC converts time and amplitude analog signal to a discreet number signal.

- **Noise** - every system generates noise. Main sources of noise are fluctuations of counts and velocities of charge carriers. We can distinguish 3 main types of noises:

  Thermal noise - generated by thermal agitation of charge carriers. Happens regardless of voltage. Reducible by cooling.

  Shot noise - volume noise. Caused by random statistical fluctuations of electric current.

  1/f noise - generated on components of circuit with resistance, such that spectral density is inversely proportional to frequency. Noise analysis is carried out by configuration of representative components in circuit.

4.3.1 β-source tests in Prague

Beta source tests also take place in Prague laboratories of IPNP on DAQload setup. DAQload is testing sensor of 1cm x 1cm silicon area. Setup consists of beta source emitting electrons through collimator with cylindrical hole in the middle. The position of beta source can be adjusted thanks to screw mounted on supporting structure. Following, this collimated stream hits detector, interacts with silicon, leaves binary signal retained in L0 pipeline, and passes through hole in aluminium frame of the test frame into scintillator. Whole setup is built inside black box preventing further outside noise, installed with heater to regulate temperature inside the black box. The mentioned setup was already shown on figure 4.4. Scintilator is composed of crystal, where electrons form beta source are detected. Crystal is connected to the photomultiplier tube. Afterwards we need to ensure compatibility of output signal from scintilator with further electronics namely ATLYS board. The process is as follows: Firstly negative analog pulse from scintilator is modified into signal compatible for ATLYS board. The analog signal is supplied to the Constant Fraction Discriminator (CFD) module that modifies signal to the digital pulse. The integral part of the setup that allows power supply and connection of modules used for signal modification consists of the Nuclear Instrumentation Module (NIM). Result of this modification is negative digital signal but given that ATLYS board utilizes positive signal another modification is needed. The Level Adapter single-width module is used for this purpose. Its ability to convert NIM logic levels to the TTL signal finally creates signal used as a external trigger for ATLYS board. Signal prepared like this is then used by readout system. Individual modifications, done by standard setup used for signal modification in Prague, are shown on figure 4.7.[28]

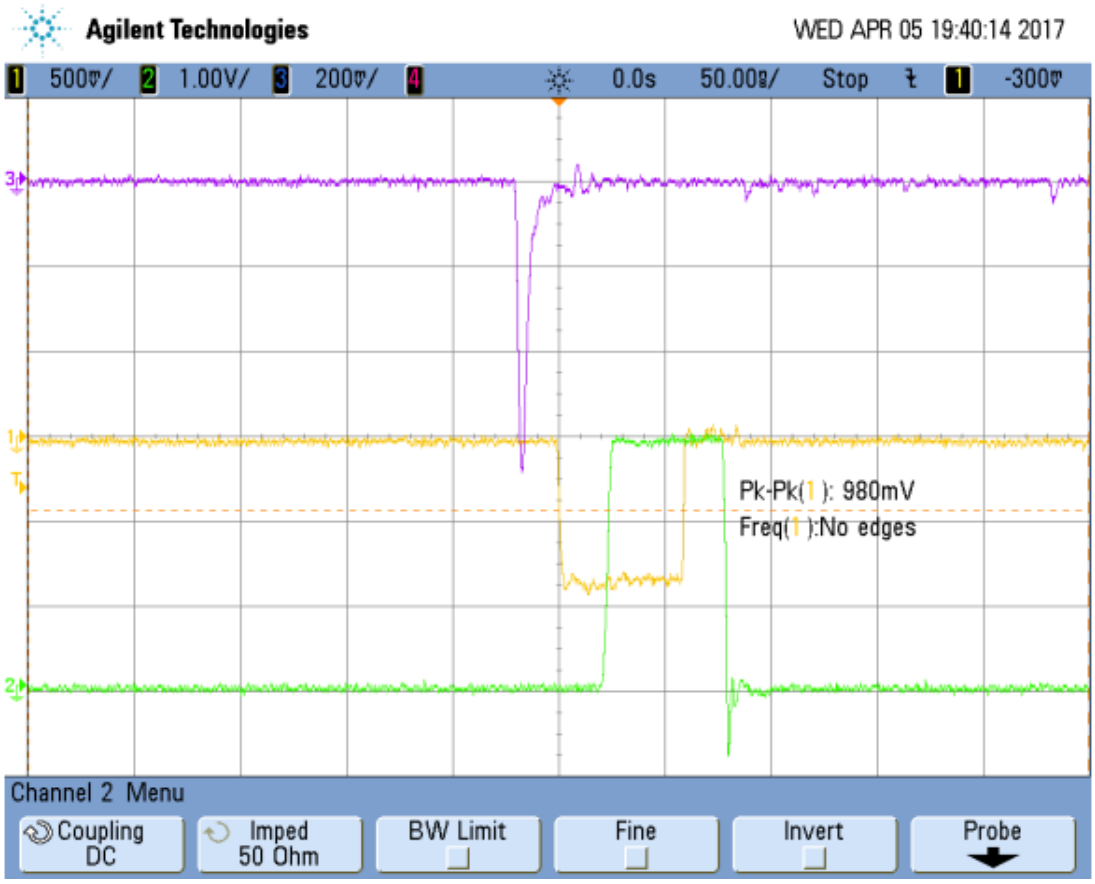

Figure 4.7: Negative analog signal from scintilator(purple), Negative digital signal from CFD(yellow), final Positive digital signal from TTL(green) [28]

Used signal modifiers are shown on figure 4.8

Figure 4.8: Signal modifiers [29]

The figure 4.9 shows diagram of described signal path.

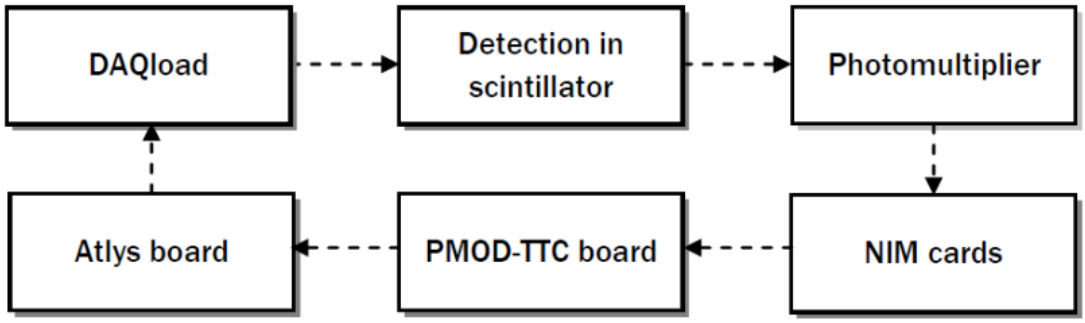

Figure 4.9: Signal path [28]

Software-ITSDAQ

Software used for data analysis is ATLAS ITk Strips DAQ (ITSDAQ). ITSDAQ runs on Windows and Linux systems in ROOT environment allowing us with parameter setting for chips. Upon running prepared program the power board of module is configured supplying the chip with power and serving as some kind of protection from high voltage resulting in increase of current. After the configuration of powerboard chips are configured resulting in further increase of current, These changes in current can serve as a control phenomenon of successful configuration. Subsequently before each test calibration of configuration is need which was further described in section 3.3. Calibration is call upon by preprogrammed macros. Full calibration of configuration consists of:

- Trimming - aims at minimizing channel-by-channel response variations. The charge of 1fC is injected into channels to find and optimal setting for each channel. This scan is done for several different DAC settings. Result of trimming is necessary shift of offset, defined as channel response for zero charge.

- Thresholds scan 3.3.1 - is done to obtain information about efficiency loss for various charges namely the Vt50 mentioned earlier in thesis.
- Strobe delay 3.3.1 - its purpose is to set a proper timing so that discriminators are in sync with the calibration signal.
- Three point gain 3.3.1 - consists of three threshold scans with different injected charge, plotted as a function, subsequently linearly fitted in order to get a conversion rate of units measured.
- Response curve 3.3.1 - consists of ten threshold scans, has the same purpose as three point gain but for higher charges where the function is no longer linear.
- Noise occupancy 3.2 - is done to determine efficiency of each channel.

Conclusion

Finally, let us summarize the thesis. The aim of this thesis was to introduce the LHC with its detectors especially ATLAS and its ongoing modernization project ATLAS Upgrade. Another goal was to describe silicon sensors used in ATLAS detector and its upgrade, and tests used to determine their properties.Firstly, the structure of ATLAS and ATLAS Upgrade were compared and described alongside with the changes in inner detector. Several phases of said upgrade were described with their goals and adjustments in each of them.

Semiconductors were introduced and principle of p-n junction and of their purpose as semiconductor detectors was explained. Afterwards, both SCT and ITk modules were described in detail and compared, also the difference in layout and position in the detector was mentioned, additionally pictures of modules in these structures were provided.

Furthermore, readout system with its trigger system and event filtering were explained with a reason for said filtering. Consequently, hardware and software for readout were outlined. Upgrade of chips used in readout was also mentioned and its influence on data flow outlined. Scans for detection characterization were explained and provided with theirs purpose.

Lastly, special tests such as laser test,beam test and β-source test were described with their applications in Prague laboratories. These tests are used to determine properties of manufactured sensors by simulating environment during collisions. Sole contribution of author lays only in gathering theoretical background and understanding of working principles. The lack of practical contribution was caused by late arrival of sensors with new chips as well as unavailability of the laboratories used for readout of old sensors. Practical contributions was supposed to lay in running the tests on new sensors with star chips.

Bibliography

[1] CERN, About CERN, online[12.12.2021]:http://home.cern/about.

[2] CERN, Large Hadron Collider, online[12.12.2021]: http://home.cern/science/accelerators/large-hadron-collider.

[3] Stefano Meroli, Machines, Projects and Experiments operating at CERN online[12.12.2021]: https://meroli.web.cern.ch/lecturemachineexperimentcern.html.

[4] JetGoodson, Search for Supersymmetry in States with Large Missing Transverse Momentum and Three Leptons including a Z-Boson, Stony Brook University, 12.5.2021, online[12.12.2021]: http://www.jetgoodson.com/blog/thesis-gallery

[5] CERN, The ATLAS detector, online[12.12.2021]: https://atlas.cern/discover/detector

[6] CERN, The Inner detector, online[13.12.2021]: https://atlas.cern/discover/detector/inner-detector

[7] ATLAS Collaboration:Technical Desing Report, Volume 1, 1999

[8] CERN, Calorimeter, online[13.12.2021]: https://atlas.cern/Discover/Detector/Calorimeter

[9] CERN, The Muon spectrometer, online[13.12.2021]: https://atlas.cern/discover/detector/muon-spectrometer

[10] CERN, Trigger and Data Acquisition, online[16.12.2021]:

https://atlas.cern/discover/detector/trigger-daq

[11] CERN, Magnet system, online[7.3.2022]: online link

[12] Vincenzo Izzo, ATLAS upgrades, Napoli, 24.9.2020, online[17.12.2021]: https://cds.cern.ch/record/2732959/files/ATL-UPGRADE-PROC-2020-001.pdf

[13] S. Rajagopalan, ATLAS Future Plans:Upgrade and the Physics with High Luminosity, The European Physical Journal Conferences, May 2013, online[14.3.2022]: online link

[14] Lingxin Meng, ATLAS ITk Pixel Detector Overview, Talk presented at the International Workshop on Future Linear Colliders, 15-18 March 2021, online[17.12.2021]: https://arxiv.org/pdf/2105.10367.pdf

[15] Shih-Chieh Hsu, ATLAS Inner Tracker (ITk) Upgrade, Hong Kong, 24.1.2018, online[17.12.2021]: https://cds.cern.ch/record/2302625/files/ATL-ITK-SLIDE-2018-073.pdf

[16] R.Nave, Intrinsic Semiconductor, online[24.2.2022]: http://hyperphysics.phy-astr.gsu.edu/hbase/Solids/intrin.html

[17] Nipun, Difference Between p-type and n-type Semiconductor, 19.10.2015online[24.2.2022]:https://pediaa.com/difference-between-p-type-and-n-type-semiconductor/

[18] M.Krammer, F.Hartmann, Silicon detectors, 2011, online[24.2.2022]: online link

[19] Y.Unno, ATLAS silicon microstrip detector system(SCT), Volume 511, Issues 1–2, 21.9.2003, online[28.2.2022]: https://www.sciencedirect.com/science/article/pii/S0168900203017510

[20] A.Ahmad, Z.Albrechtskirchinger, P.P.Allport, ..., The silicon microstrip sensors of the ATLAS semiconductor tracker, Volume 578, Issue 1, 21.7.2007, online[28.2.2022]: https://www.sciencedirect.com/science/article/pii/S0168900207007644

[21] A.Abdesselam, P.J.Adkin, P.P.Allport, ..., ATLAS SCT End-Cap Module Production, 21.9.2006 online[29.4.2022]: https://cds.cern.ch/record/973395/files/indet-pub-2006-007.pdf

[22] J.Fernández-Tejero, Design and Optimization of Advanced Silicon Strip Detectors for High Energy Physics Experiments, July 2020, online[11.4.2022]:https://www.researchgate.net/figure/Computer-generated-image-of-an-End-cap-Petal-housing-six-different-End-cap-stripfig10343206500

[23] TDR for ATLAS Inner Tracker Strip Detector, online[4.5.2022]: http://cds.cern.ch/record/2257755/

[24] B.J.Rosser, Verification of Readout Electronics in the ATLAS ITk Strips Detector, Talk presented at the 2019 Meeting of the Division of Particles and Fields of the American Physical Society, July 29–August 2, 2019, Northeastern University, Boston, online[21.3.2022]:https://arxiv.org/pdf/1910.06694.pdf

[25] F.M.N., F.A, J.K, ABC130 ASIC Specification v4.5, 30.4.2013, online[23.3.2022]:online link

[26] L. Poley, The ABC130 barrel module prototyping programme for the ATLAS strip tracker, 2020, online[24.3.2022]:http://uu.diva-portal.org/smash/get/diva2:1499503/FULLTEXT01.pdf

[27] W.Lu, F.Anghinolfi, L.Cheng, Development of the ABC-Star front-end chip for the ATLAS silicon strip upgrade,

online[24.3.2022]:https://www.researchgate.net/figure/From-ABC130-HCC130-to-ABCStar-HCCStarfig3316266824

[28] M.Sýkora, Tests of Semiconductor Detectors for ATLAS Upgrade, Master thesis, Charles University 2017

[29] O.Kovanda, Beta Source tests of Semiconductor Detectors ITk for ATLAS Upgrade, Master thesis, Charles University 2019

[30] Z.Doležal, P.Kodyš, P.Řezníček, J.Brož, P.Bažant, P.Kvasnička, Laser tests of ATLAS SCT modules, online[28.4.2022]: https://ipnp.cz/ kodys/works/lasertest/Tests2006/tests082006.html

[31] P.Krásny, Tests of Semiconductor Detectors in Prague Laboratory, Bachelor thesis, Charles University 2019

[32] Z.Doležal, Polovodičové detektory v jaderné a subjaderné fyzice), online[3.4.2022]:https://ipnp.cz/ dolezal/teach/semicon/semip.pdf

List of Figures

List of Abbreviations

ABC ATLAS Binary Chip
ADC Analog to DIgital Converter
ALICE A Large Ion Collider Experiment
ASIC Application Specific Integrated Circuit
ATLAS A Toroidal LHC Apparatus
BC Bunch Crossing
CERN Conseil Européen pour la Recherche Nucléaire
CFD Constant Fraction Discriminator
CMS Compact Muon Solenoid
DAC Data Acquisition counts
DAQ Data Acquisition
DUT Device Under Test
EF Event Filter
EM Electromagnetic calorimeters
FE Front-end
FELIX Front-End Link exchange
HCC Hybrid Controller Chip
ID Inner Detector
innse input noise
ITk ATLAS Inner Tracker upgrade
ITSDAQ ATLAS ITk Strips Data Acquisition
LAr Liquid Argon calorimeter
LHC Large Hadron Colider
LHCb Large Hadron Collider beauty
NIM Nuclear Instrumentation Module
NO Noise Occupancy
outnse output noise
ROB Readout Buffer
ROI Region of Interest
SCT Semiconductor Tracker
SCTDAQ Semiconductor Tracker Data Acquisition
SNR Signal-to-noise ratio
TDAQ Trigger and Data acquisition
TPG Thermal Pyrolytic Graphite
TRT Transition Radiation Tracker
TTL Transistor-Transistor Logic